Louisiana Water Resources Research Institute
Annual Technical Report
FY 2011

Introduction

This report presents a description of the activities of the Louisiana Water Resources Research Institute for the period of March 1, 2011 to February 28, 2012 under the direction of Dr. John Pardue. The Louisiana Water Resources Research Institute (LWRRI) is unique among academic research institutions in the state because it is federally mandated to perform a statewide function of promoting research, education and services in water resources. The federal mandate recognizes the ubiquitous involvement of water in environmental and societal issues, and the need for a focal point for coordination.

As a member of the National Institutes of Water Resources, LWRRI is one of a network of 54 institutes nationwide initially authorized by Congress in 1964 and has been re-authorized through the Water Resources Research Act of 1984, as amended in 1996 by P.L. 104-147. Under the Act, the institutes are to:

"1) plan, conduct, or otherwise arrange for competent research that fosters, (A) the entry of new research scientists into water resources fields, (B) the training and education of future water scientists, engineers, and technicians, (C) the preliminary exploration of new ideas that address water problems or expand understanding of water and water-related phenomena, and (D) the dissemination of research results to water managers and the public.

2) cooperate closely with other colleges and universities in the State that have demonstrated capabilities for research, information dissemination and graduate training in order to develop a statewide program designed to resolve State and regional water and related land problems. Each institute shall also cooperate closely with other institutes and organizations in the region to increase the effectiveness of the institutes and for the purpose of promoting regional coordination."

The National Water Resources Institutes program establishes a broad mandate to pursue a comprehensive approach to water resource issues that are related to state and regional needs. Louisiana is the water state; no other state has so much of its cultural and economic life involved with water resource issues. The oil and gas industry, the chemical industry, port activities, tourism and fisheries are all dependent upon the existence of a deltaic landscape containing major rivers, extensive wetlands, numerous large shallow water bays, and large thick sequences of river sediments all adjacent to the Gulf of Mexico.

History of the Institute

Louisiana has an abundance of water resources, and while reaping their benefits, also faces complex and crucial water problems. Louisiana’s present water resources must be effectively managed, and the quality of these resources must be responsibly protected. A fundamental necessity is to assure continued availability and usability of the state's water supply for future generations. Specifically, Louisiana faces five major issues that threaten the quality of the state’s water supply, which are also subsets of the southeastern/island region priorities:

Nonpoint sources of pollution are estimated to account for approximately one-half of Louisiana's pollution. Because of the potential impact of this pollution and the need to mitigate its effects while maintaining the state's extensive agricultural base and coastal zones, continued research is needed in the area of nonpoint issues. Louisiana’s regulatory agencies are addressing non-point source problems through the development of waste load allocation models or total maximum daily load (TMDL) calculations. There are serious technical issues that still require resolution to insure that progress is made in solving the non-point source problem.

Louisiana's vast wetlands make up approximately 40% of the nation's wetlands. These areas are composed of very sensitive and often delicately balanced ecosystems which make them particularly vulnerable to

contamination or destruction resulting both from human activities and from natural occurrences. Understanding these threats and finding management alternatives for the state's unique wetland resources are priority issues needing attention.

Water resources planning and management are ever-present dilemmas for Louisiana. Severe flooding of urban and residential areas periodically causes economic loss and human suffering, yet solutions to flooding problems can be problems in themselves. Water supply issues have also recently a focus of concern. Despite the abundance of resources, several aquifers have been in perennial overdraft, including the Chicot aquifer. Louisiana passed its first legislation that restricts groundwater use in the past year. Water resources and environmental issues are intricately interconnected; therefore, changes in one aspect produce a corresponding responsive change in another. Further study is needed to understand these relationships.

Water quality protection, particularly of ground water resources, is an area of concern in Louisiana. Researchers are beginning to see contamination in drinking water supplies that was not present in the past. Delineating aquifer recharge areas, understanding the impacts of industrial activities on water resources, evaluating nonpoint sources of pollution, and exploring protection alternatives are issues at the forefront.

Wastewater management has been a long-standing issue in Louisiana. The problem of wastewater management focuses primarily on rural and agricultural wastewater and the high costs for conventional types of wastewater treatment as found in the petrochemical industry.

The Institute is administratively housed in the College of Engineering and maintains working relationships with several research and teaching units at Louisiana State University. Recent cooperative research projects have been conducted with the University of New Orleans and the EPA’s Hazardous Substance Research Center- South & Southwest.

Research Program Introduction

The primary goal of the Institute is to help prepare water professionals and policy makers in the State of Louisiana to meet present and future needs for reliable information concerning national, regional, and state water resources issues. The specific objectives of the Institute are to fund the development of critical water resources technology, to foster the training of students to be water resources scientists and engineers capable of solving present and future water resources problems, to disseminate research results and findings to the general public, and to provide technical assistance to governmental and industrial personnel and the citizens of Louisiana.

The priority research areas for the Institute in FY 2011 focused on selected research themes developed in conjunction with the advisory board. These themes corresponded to the major water resource areas affecting Louisiana described in the Introduction above. Projects selected were from a range of faculty with different academic backgrounds including geological scientists, environmental engineers and water resource engineers and scientists. Supporting research in these priority areas has increased the visibility of the Institute within the State.

The individual research projects designated as Projects 2011LAXXXX, are listed below.

•Project 2010LA76G, Tsai & Hanor - Hierarchical Multimodel Saltwater Intrusion Remediation and Sampling Designs: A BMA Tree Approach

•Project 2011LA79B-Willson Development of a 2D Hydrodynamic Model of the Mississippi River and Application To Long-Term Management Scenarios, Contaminant Transport and Sediment Transport •Project 2011LA80B- Deng. Louisiana Watershed Education Initiative for Environmental Sustainability •Project 2011LA81B- Tsai, Feasibility Study of Scavenging Approach to Stop Saltwater Toward Water Wells

•Project 2011LA82B--Smith, Turbulent Interactions of Coastal Vegetation and Waves

These projects include two projects that focus on climate and hydrologic processes (Project 2011LA79B and Project 2011LA82B), one project that focus on groundwater (Project 2011LA81B), and one project that focuses on education (Project 2011LA80B)

Hierarchical Multimodel Saltwater Intrusion Remediation and Sampling Designs: A BMA Tree Approach

Basic Information

Title:	Hierarchical Multimodel Saltwater Intrusion Remediation and Sampling Designs: A BMA Tree Approach
Project Number:	2010LA76G
Start Date:	9/1/2010
End Date:	8/31/2013
Funding Source:	104G
Congressional District:	Louisiana
Research Category:	Ground-water Flow and Transport
Focus Category:	Groundwater, Management and Planning, Methods
Descriptors:	None
Principal Investigators:	Frank Tsai, Jeff Hanor

Publications

1. Tsai, F.T.-C. (2011). Scavenger Wells Stop Saltwater Intrusion in Baton Rouge, Louisiana, IGWMC MODFLOW and More 2011 Conference: Integrated Hydrologic Modeling, Golden, Colorado, June 5-8, 2011.
2. Tsai, F. T.-C., and Ahmed S. Elshall (2011). A Hierarchical Bayesian Model Averaging Approach to Cope With Sources of Uncertainty in Conceptual Ground Water Models, World Water & Environmental Resources Congress, Palm Springs, California, May 22-26, 2011.
3. Tsai, F. T.-C. (2011). Stop Saltwater Intrusion Toward Water Wells Using Scavenger Wells, World Water & Environmental Resources Congress, Palm Springs, California, May 22-26, 2011.
4. Callie E. Anderson and Jeffrey S. Hanor (2011) Origin of waters causing salinization of the Baton Rouge aquifer system, Louisiana. South-Central Section Geological Society of America 45th Annual Meeting, March 27-29, 2011.
5. Frank T.-C. Tsai (2011). Saltwater Intrusion Simulation in the “1,500-Foot” Sand of the Baton Rouge Area: Pre-Anthropogenic Pumping, Current Situation, Future, Fifth Annual Louisiana Groundwater, Coastal Geology and Subsidence-Land Loss Symposia, Baton Rouge, Louisiana, January 11-12, 2011.
6. Callie E. Anderson and Jeffrey S. Hanor (2011) The St. Gabriel salt dome as a potential source of the salty waters contaminating the Baton Rouge aquifer system. Fifth Annual Louisiana Groundwater, Coastal Geology and Subsidence-Land Loss Symposia, Baton Rouge, Louisiana, January 11-12, 2011.
7. Ahmed Elshall and Frank T.-C. Tsai (2011). Geophysical and geostatistical approaches to subsurface characterization of the Baton Rouge area, Fifth Annual Louisiana Groundwater, Coastal Geology and Subsidence-Land Loss Symposia, Baton Rouge, Louisiana, January 11-12, 2011.
8. Nima Chitsazan and Frank T.-C. Tsai (2011). Bed boundary delineation of “1,500-foot’, “1,700-foot”, and “2,000-foot sands of the Baton Rouge area, Fifth Annual Louisiana Groundwater, Coastal Geology and Subsidence-Land Loss Symposia, Baton Rouge, Louisiana, January 11-12, 2011.
9. Tsai, F. T.-C. (2010). “1,500-Foot” Sand Saltwater Intrusion Simulation and Management Using Scavenger Wells, Baton Rouge Geological Society, Baton Rouge, Louisiana, December 10, 2010. (invited)

10. Tsai, F.T.-C. (2010), Scavenger Wells Stop Saltwater Intrusion in Baton Rouge, 2010 Louisianan Water Quality Technology Conference, Alexandria and Baton Rouge, Louisiana, December 14-15, 2010. (invited)
11. Tsai, F.T.-C. (2010) Scavenger Well Operation to Stop Saltwater Intrusion Toward BRWC Lula Wells in the Baton Rouge Area, Louisiana Capital Area Ground Water Conservation Commission, September 14, 2010. (invited)
12. • Frank Tsai, 2012, Feasibility Study of Scavenging Approach to Stop Saltwater Toward Water Wells, Louisiana State University, Baton Rouge, Louisiana, 10 pages. (USGS 104B)
13. Tsai, F. T.-C., and A.S. Elshall. (2011). A Hierarchical Bayesian Model Averaging Approach to Cope With Sources of Uncertainty in Conceptual Ground Water Models, World Water & Environmental Resources Congress, Palm Springs, CA, May 22-26, 2011.
14. Tsai, F. T.-C. (2011). Development of Scavenger Well Operation Model To Stop Saltwater Intrusion Toward Water Wells In The “1,500-Foot” Sand of The Baton Rouge Area, Louisiana, World Water & Environmental Resources Congress, Palm Springs, CA, May 22-26, 2011.
15. Tsai, F. T.-C. (2011). Scavenger Wells Stop Saltwater Intrusion in Baton Rouge, Louisiana, MODFLOW and More 2011, Golden, CO, June 5-8, 2011

SYNOPSIS

Title: Hierarchical Multimodel Saltwater Intrusion Remediation and Sampling Designs: A BMA Tree Approach
Project Number: G10AP00136
Start Date: 9/1/2010
End Date: 8/31/2013
Funding Source: 104G
Research Category: Ground-water Flow and Transport
Focus Categories: GW, M&P, MET
Descriptors: Remediation Design, Sampling Design, Saltwater Intrusion, Optimization, Uncertainty
Primary PI: Frank T.-C. Tsai
Other PI: Jeffrey S. Hanor

Problem and Research Objectives

Water use in Baton Rouge, Louisiana is approximately 629,000 m^3 per day (166 million gallons per day) out of which 88% is ground water and the rest is surface water (Sargent, 2007). Due to excessive ground water pumping, saltwater is intruding from the saline aquifers in the south part of the Baton Rouge Fault. Thus, in the absence of any remediation measure, some of public supply water wells in East Baton Rouge Parish are under the threat of being abandoned in the near future. The project objective is to develop saltwater intrusion models to be employed for the management and remediation of the ground water resources for the study area shown in Figure 1. The study area is approximately 500 km^2. To ensure a valid saltwater intrusion model, the interim report develops stratigraphy models that capture the complexity and heterogeneity of the subsurface geology in the Baton Rouge area.

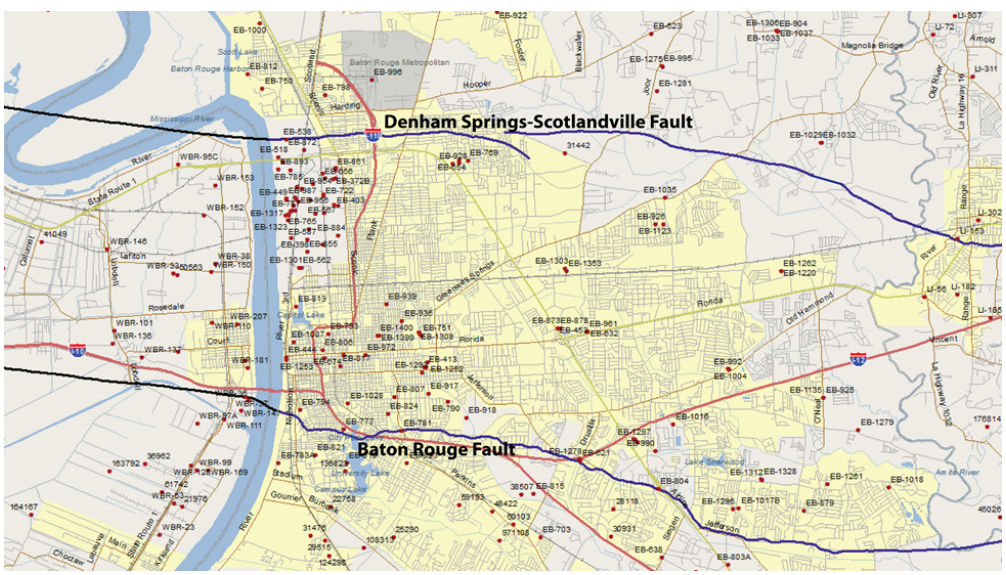

Figure 1: The study area. Red dots are electrical logs. The base map is created by Louisiana GIS Digital Map 2007. The fault lines are obtained from McCulloh and Heinrich (2012).

Due to limited amount of data and since model uncertainty always exists, multiple models are usually developed. Model selection, model elimination, model reduction, and model discrimination are commonly used to select the best model. It is clear that modeling uncertainty is always underestimated if only the best model is used. One would ask why only the best model is used afterwards when so many efforts have been devoted to calibrating many models. This certainly wastes valuable resources and important information from other good models. Hierarchical Bayesian model averaging (HBMA) best utilize all possible models for model prediction and application under Bayesian statistical framework. HBMA presents several advantages over model selection: (1) Information from all possible models is used based on their model importance (model weights). Calibration efforts are not wasted. (2) The model importance is based on the evidence of data, which avoids over-confidence in the best model that does not have a dominant model weight. And (3) model structure uncertainty is increased and is better presented than that by using a single model. Moreover, HBMA is able to distinguish model uncertainty arising from individual models and between models. HBMA is able to identify unfavorable models even though they may present small prediction uncertainty.

In this study, HBMA is used to construct stratigraphy for the Baton Rouge aquifer system. Indicator geostatistical techniques are used to analyze electrical resistivity logs and reconstruct the subsurface accordingly. The HBMA is applied to analyze the conceptual model structure uncertainty arising from the different sand-clay line cutoff values for the resistivity logs and the different sand-clay cutoff probabilities for the interpolated values.

Methodology

(1) Indicator Kriging

Given the volumetric domain $D \subset \mathbb{R}^n$, the indicator function $\{I(\boldsymbol{x}, v) : \boldsymbol{x} \in D\}$ is a random function. The indicator random variable v describes the spatial extension of a categorical variable C, which is the sand-clay distribution in aquifers under different sand-clay line cutoff $\propto$ as determined from the electrical resistivity logs. The random function of the indicator random variable of class *C* is defined as:

$$I(\boldsymbol{x}, v) = \begin{Bmatrix} 1 \;\; v \in C\,, \;\; v(\boldsymbol{x}) > \propto \\ 0 \;\; v \;\notin C, \qquad v(\boldsymbol{x}) < \propto \end{Bmatrix} \tag{1}$$

where *I*=1 is sand and *I*=0 is clay in this study. The indicator function $I(\boldsymbol{x}, v)$ is a random function of two variables in which v is an outcome of random variable at location $\boldsymbol{x}$ in which the one and zero indicates the presence of sand and clay, respectively. The indicator variogram has the same definition as the normal variogram except that the real random function is replaced by the indicator random function $I(x)$ as follows

$$\gamma_{I}(h) = \frac{1}{2N(h)} \sum_{i=1}^{N(h)} [I(x_i - I(x_i + h)]^2 \tag{2}$$

where $N(h)$ is the number of pairs within the lag interval h. The main source of the sample data, which are used to generate the IK variograms, is from the electrical resistivity logs that are provided by the Louisianan Department of Natural Resources (DNR), the Department of Transportation and Development (DOTD), the United States Geological Survey (USGS), the Louisiana Geological Survey (LGS), and the Baton Rouge Water Company (BRWC). In the study area shown in Figure 1, we have more than 350 electrical logs.

For each foot and for every resistivity log location, the resistivity values indicate either sand or clay depending on the sand-clay line cutoff as determined from the clay line in the resistivity

curves. Another source of data is from the study of Wendeborn and Hanor (2008), in which they analyzed spontaneous potential (SP) curves to identify the sand-clay distribution along the Baton Rouge fault. The interpretation of these logs in terms of sand-clay sequences are amended to the main data to provide more sampling locations. All observation points are amended together through linear interpolation over each foot. The number of samples in each observation point varies from 800 to 3000 depending on the depth of each borehole. Thus, over a depth z with an increment of 1 foot, an experimental variogram is generated. A pseudo 3D horizontal experimental variogram is obtained by averaging all the 2D experimental variograms for all depths.

Under the basic assumption that the sample domain is stationary, ergodic and sufficient to reliable reproduce the statistics, the obtained theoretical variogram is used for the indicator kriging interpolation as a method for constructing the subsurface stratigraphy. The aim of kriging is to estimate the value of a random variable at unsampled points. Over a defined cell size, which is $200\,m \times 200\,m$ in this study, indicator kriging uses weighted average of the neighboring sample data points to estimate the indicator value in each cell using the following system of equations:

$$\begin{bmatrix} \gamma(x_1,x_1) & \gamma(x_1,x_2) & \mathrm{L} & \gamma(x_1,x_N) & 1 \\ \gamma(x_2,x_1) & \gamma(x_2,x_2) & \mathrm{L} & \gamma(x_2,x_N) & 1 \\ \mathrm{M} & \mathrm{M} & \mathrm{L} & \mathrm{M} & \mathrm{M} \\ \gamma(x_N,x_1) & \gamma(x_N,x_2) & \mathrm{L} & \gamma(x_N,x_N) & 1 \\ 1 & 1 & \mathrm{L} & 1 & 0 \end{bmatrix} \begin{bmatrix} \lambda_1 \\ \lambda_2 \\ \mathrm{M} \\ \lambda_N \\ L \end{bmatrix} = \begin{bmatrix} \gamma(x_1,x_0) \\ \gamma(x_2,x_0) \\ \mathrm{M} \\ \gamma(x_N,x_0) \\ 1 \end{bmatrix} \text{ or } A\lambda = b \tag{3}$$

in which $\gamma(x_i, x_j)$ is the variogram of v between the data points x_i and x_j , and the $\gamma(x_i, x_o)$ is the variogram between the data point x_i and the target point x_o. To guarantee that the estimates are unbiased, the sum of the weights λ_i is one. The unbiased constrained is imbedded to the minimization problem through the use of the Lagrange multiplier L. Once the weights for each data point are obtained, the last step is to calculate the expected indicator value and the indicator kriging variance by using the following equations.

$$v^*(x_0) = \sum_{i=1}^{N} \lambda_i I(x_i) \quad and \quad \sigma_{IK}^2 = b^T \lambda \tag{4}$$

(2) Hierarchical Bayesian Model Averaging (HBMA)

To cope with sources of uncertainty in stratigraphy models, a hierarchical Bayesian model averaging is developed. Consider $\mathrm{M}_{\underbrace{(\mathrm{ij...lm})}_{\mathrm{p}}} \in \mathbf{M}_{\mathrm{p}}$ a model at level p. The subscript $\underbrace{(\mathrm{ij\ ...\ lm})}_{\mathrm{p}}$ locates the model hierarchically top down from the first level, to the second level and so forth to reach to level p. For example, $\mathrm{M}_{(\mathrm{i})} \in \mathbf{M}_1$ is model i at level 1, $\mathrm{M}_{(\mathrm{ij})} \in \mathbf{M}_2$ is model j at level 2, which is a child model to parent model i at level 1. $\mathrm{M}_{(\mathrm{ijk})} \in \mathbf{M}_3$ is model k at level 3, which is a child model to the parent model j at level 2 and the grandparent model of model i at level 1. From bottom up, parent models $\mathbf{M}_{\mathrm{p}-1}$ at level $\mathrm{p}-1$ is composed of the child models $\mathbf{M}_{\mathrm{p}}$ at level p. Models $\mathbf{M}_{\mathrm{p}-2}$ at level $\mathrm{p}-2$ are composed of models $\mathbf{M}_{\mathrm{p}-1}$ at level $\mathrm{p}-1$ and so forth until the Hierarch BMA model M_0 is reached.

Consider base models at level p. According to the law of total probability, the posterior probability for predicted quantity Δ given data $\mathbf{D}$ is

$$\Pr(\Delta \mid \mathbf{D}) = E_{\mathbf{M}_1} E_{\mathbf{M}_2} \mathrm{L}\ E_{\mathbf{M}_p}\left[\Pr(\Delta \mid \mathbf{D}, \mathbf{M}_p)\right] \tag{5}$$

where $E_{\mathbf{M}_p}$ is the expectation operator with respect to models $\mathbf{M}_p$ at level p. $\Pr(\Delta|\mathbf{D}, \mathbf{M}_p)$ is the posterior probability of predicted quantity Δ given data $\mathbf{D}$ and models $\mathbf{M}_p$ at level p. The expectation $E_{\mathbf{M}_p}[\Pr(\Delta|\mathbf{D}, \mathbf{M}_p)]$ is posterior probability averaging at level p. That is

$$E_{\mathbf{M}_p}\left[\Pr(\Delta \mid \mathbf{D}, \mathbf{M}_p)\right] = \sum_m \Pr\left(\Delta \mid \mathbf{D}, \underbrace{M_{(ijL,\ lm)}}_{p}\right) \Pr\left(\underbrace{M_{(ijL,\ lm)}}_{p} \mid \mathbf{D}, \underbrace{M_{(ijL,\ l)}}_{p-1}\right). \tag{6}$$

where $\Pr\left(\Delta \mid \mathbf{D}, \underbrace{M_{(ijL,\ lm)}}_{p}\right) = \Pr(\Delta \mid \mathbf{D}, \mathbf{M}_p)$.

$\Pr\left(\underbrace{M_{(ijL,\ lm)}}_{p} \mid \mathbf{D}, \underbrace{M_{(ijL,\ l)}}_{p-1}\right) = \Pr(\mathbf{M}_p \mid \mathbf{D}, \mathbf{M}_{p-1})$ is the conditional posterior model probability of model $\underbrace{M_{(ij\ldots lm)}}_{p}$ at level p under model $\underbrace{M_{(ij\ldots l)}}_{p-1}$ at level $p-1$. $\Pr(\mathbf{M}_p \mid \mathbf{D}, \mathbf{M}_{p-1})$ also represents the conditional model weights and will be used to develop a BMA tree of model weights. Note that model $M_{(ij\ldots lm)}$ is a child model under the parent model $M_{(ij\ldots l)}$ because both have the same subscript for the first $p-1$ levels. Equation (6) is the Bayesian model averaging (BMA) at level p, which can be written as

$$\Pr(\Delta \mid \mathbf{D}, \mathbf{M}_{p-1}) = E_{\mathbf{M}_p}\left[\Pr(\Delta \mid \mathbf{D}, \mathbf{M}_p)\right] \tag{7}$$

According to equations (5) and (7), one can derive the posterior probability of prediction using BMA over models at any level, say level n:

$$\Pr(\Delta \mid \mathbf{D}, \mathbf{M}_n) = E_{\mathbf{M}_{n+1}} E_{\mathbf{M}_{n+2}} \mathrm{L}\ E_{\mathbf{M}_p}\left[\Pr(\Delta \mid \mathbf{D}, \mathbf{M}_p)\right]. \tag{8}$$

Based on equation (8), the law of total expectation and the law of total variance, the prediction mean, within-model variance, between model variance and total variance can be derived at level n.

In this study, Δ is the indicator value and **D** is drillers logs to be used to calibrate stratigraphy model parameters.

Principal Findings and Significance

(1) Stratigraphy model calibration

For results and discussion, we use the following short forms. The first level of uncertainty has three propositions, which are Exponential (Exp), Gaussian (Gus) and Pentspherical (Pen) variogram models. The second level has global (G) and local (L) stationarity assumptions. The third level has the calibration data set with an interpretation favoring more sand (D1) or more clay (D2). The fourth level of uncertain has the geological conceptualization with respect to the Denham Springs-Scotlandville Fault resulting into two zones (Z2) or three zones (Z3) model. For example, Z3D1LExp is the name of a model with three subdomains (Z3), using the first calibration data set (D1), local stationarity assumption (L) and Exponential variogram model

(Exp).

To account for all the modeling propositions, we calibrated 24 models for the IK sand-clay cut-off ratio and the dipping angle for horizontal correlation. The best model is Z3D1LExp. The minimum, mean and maximum cut-off ratios of the 24 models are 0.3879, 0.4092 and 0.4389 respectively. These ratios are in agreement with the 0.402±0.0013 mean estimated sand ratio of the 24 models, and the calculated sand ratios from the driller logs data set 1, driller logs data set 2 and resistively logs being 0.3731, 0.4041 and 0.395 respectively. Unlike previous IK studies [Johnson and Dreiss, 1989; Falivene, 2007], which consider at cut-off ratio of 0.5 as a reasonable assumption, this study shows that cut-off ratio can be viewed as probabilities of occurrence as suggested by Chiles and Delfiner [1999], and that a fixed cut-off 0.5 may result in over and under estimation. The calibration results of the 24 models show minimum, mean and maximum dipping angle percentages to be 0.30, 0.56 and 0.79 respectively. This agrees with the geological assumption that the aquifer system is dipping southward [Griffith 2003]. The mean dipping angle and range are in good agreement with the 0.52% dipping angle as estimated from the geophysical logs of boreholes BR-1268 and BR-1028 in the BB' cross section in Griffith [2003].

Figure 2 shows the stratigraphy of the "1,200-foot", "1,500-foot", "1,700-foot" and "2,000-foot" sands between the Denham Springs-Scotlandville Fault and the Baton Rouge Fault for the best model, Z3D1LExp. To verify the correctness of the stratigraphy, we plot municipal and industrial pumping wells and USGS observation wells into the figure and confirm that all the screen intervals are in the sand portion. Figure 2 demonstrates the first time ever that we are able to understand the Baton Rouge aquifer system in detail. From Figure 2, the "1,200-foot", "1,500-foot", and "1,700-foot" interconnect in the area close to the Baton Rouge Fault. Figure 2 also shows four sands between the "1,200-foot" sand and "2,000-foot" sand. There is a distinct clay bed separates the "2,000-foot" sand from its overlying sand. Figure 2 also allows us to verify USGS well naming, facilitate determination of new monitoring wells, and locate proper depth for remediation designs.

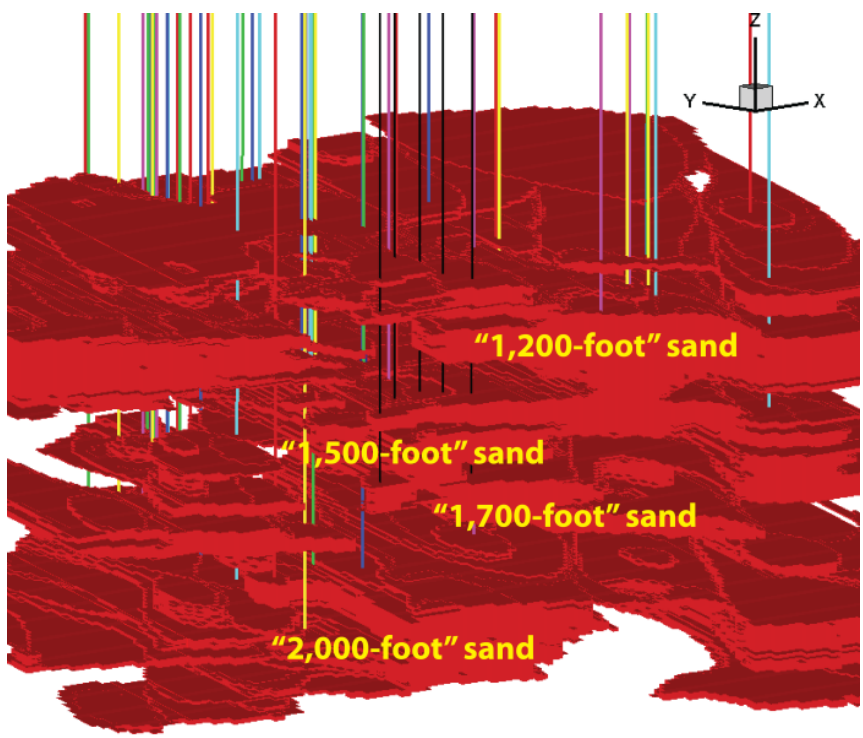

Figure 2: Stratigraphy of the "1,200-foot", "1,500-foot", "1,700-foot" and "2,000-foot" sands between the Denham Springs-Scotlandville Fault and the Baton Rouge Fault. The vertical lines are pumping wells and USGS observation wells.

Using the best model, Figure 3 shows the stratigraphy of the Baton Rouge Fault (BR Fault) and the Denham Springs-Scotlandville Fault (DSS Fault) for the northern face and the southern face. Juxtaposition of the two faces immediately locates the possible leaky areas for the Baton Rouge Fault to allow saltwater to encroach into the freshwater aquifers. Due to large downthrow, sand connection through the Baton Rouge Fault is limited. However, it is clear to see that there is an enormous area that the "1,500-foot" sand north of the Baton Rouge Fault connects the "1,200-foot" sand south of the fault. The leaky area of the Baton Rouge Fault for the "2,000-foot" sand is very small. This may explain why saltwater intrusion in the "1,500-foot" sand is much severer than in the "2,000-foot" sand. The Denham Springs-Scotlandville Fault shows better hydraulic connection through the fault.

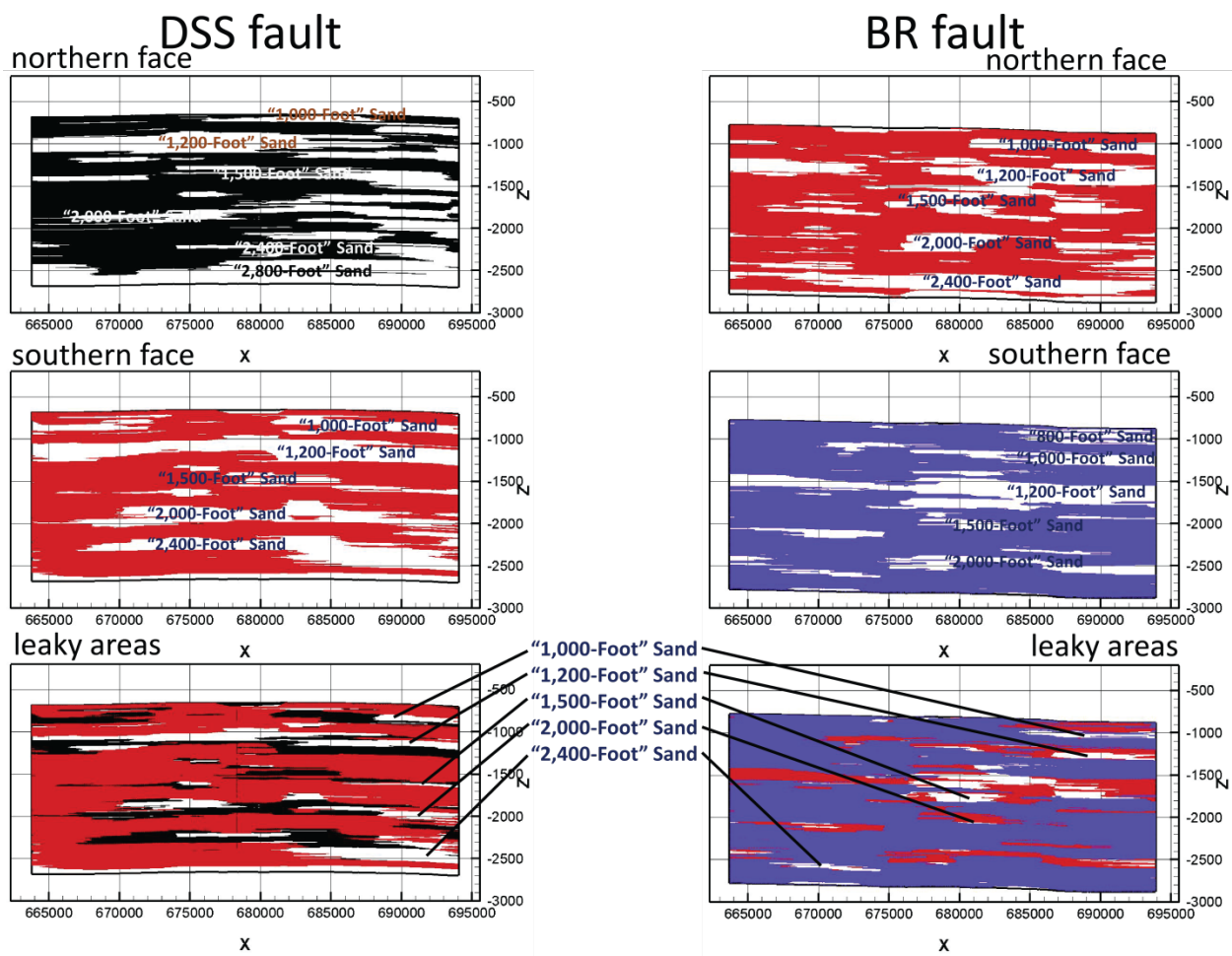

Figure 3: Stratigraphy of the Baton Rouge Fault and the Denham Springs-Scotlandville Faults. Blank areas are sands. The leaky areas through the faults are identified by juxtaposing the northern face and the southern face of the fault stratigraphy.

(2) Model weights

We calculate the model weights using both Occam's widow and different variance windows. The best model has the BIC_{min} being 3.707×10^4. The numbers of data points are 31500. Due to the large data size, the Occam's window as expected singles out only the best model. Tsai and Li [2008b] provide a table for the scaling factors for 1% and 5% significance levels for three σ_D,

which are used here. Model weights of less influential models increase as the significance levels and number of sigma increase that consecutively decrease the weights of the significant the models. Model Z3D1LExp shows to be the only significant model since it only decreased in weight, while all other models increased under all the variance windows.

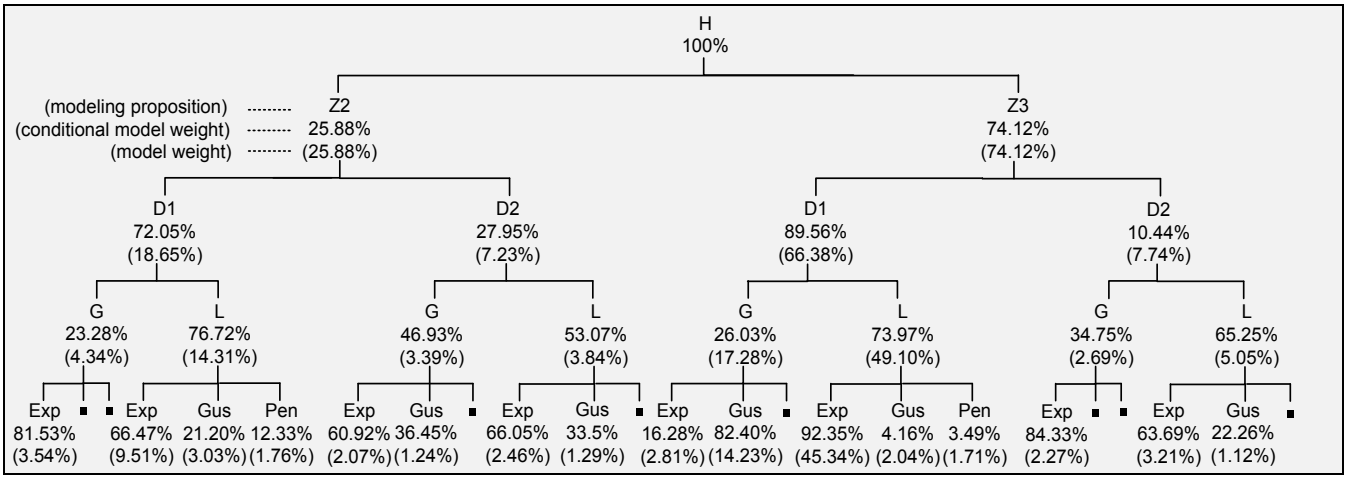

Figure 4. The BMA tree of model weights and conditional model weights for 24 models. Dots present models with model weight less than 1%.

The BMA tree of model weights and conditional model weights for 24 models is shown in Figure 4. The best model is Z3D1LExp, which has a model weight of 45.34%. Exponential models generally tend to perform better than the Gaussian and Pentspherical models, which tend to show similar results. Other modeling propositions of model Z3D1LExp, which are local stationarity (L), first data set (D1) and three subdomains (Z3), tend perform better than other competing propositions. As expected, the worst model is Z2D2GPen, which does not share a single proposition with the best model. The second worst model Z2D2LPen shares only local stationarity (L) proposition with the best model.

(3) Uncertain propagation

Smaller variance windows can be used when one is certain that only the best model is the significant model. Large variance windows are used when this is not intuitively clear and to avoid underestimating the variance. For our purpose, we use large variance window of 5% with 3σ to increase the variance estimation to clearly understand the variance propagation of the within model variance (WMV), between model variance (BMV) and total model variance (TMV). The total uncertainty at each level as expressed by the TMV is the summation of the BMV and WMV at this level. For this purpose, we present a 2D cross section of the south side of the DSS fault with a grid spacing of 50 m in the horizontal direction and 1 foot (0.304 m) in the vertical direction. The X-axis of all the plots is in [m] to agree with UTM-NAD83 coordinate system and the Y-axis is in [foot] to agree with the aquifer nomenclature in the study region.

To better understand the uncertainly propagation, we discuss the WMV, BMW and TMV for the branch of the best model starting with Z3D1L model at level one followed by Z3D1 model at level two , Z3 model at level three and HBMA model at level four. The four plots in Figure 5 show the BMV for the four uncertainty levels, which illustrates the previous remark that the BMV at a certain level is independent from the BMV at other levels. Another remarkable

observation is that the Z3D1L Z3D1 and Z3 BMA models have similar uncertainly patterns, yet with different values. The similar uncertainly patterns indicate again that the best model is dominating the BMV. Different values indicate the importance of different propositions at different level. This means that local and global variogram models are both good propositions as indicated by the high BMV values of Z3D1. On the other hand, the low BMV of Z3 indicates that the using different calibration data sets, which results in different dipping angle and cut-off values, has small impact on uncertainty. By comparing Z3D1L, Z3D1 and Z3 models with the HBMA model, we observe different pattern of uncertainty. This shows that the two subdomains and three subdomains propositions produces relatively different estimations, which is depicted in Figure 5.

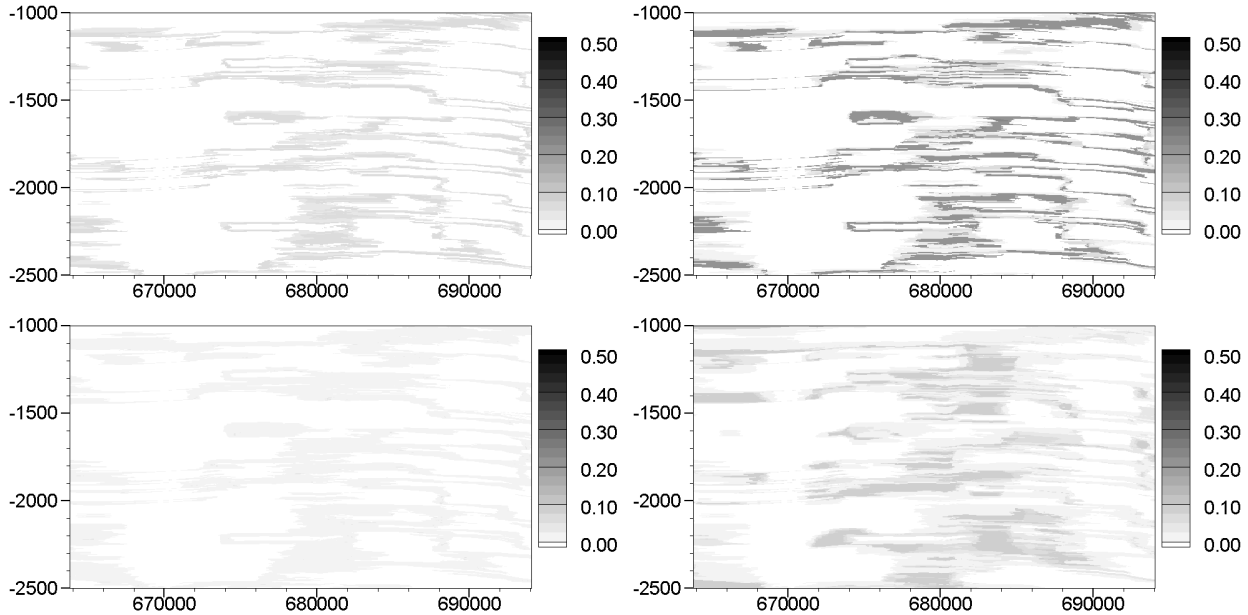

Figure 5. BMV at south side of DSS fault for BMA models Z3D1L, Z3D1, Z3 and HBMA

The WMV at the first level averages the IK variance of all sub-models in each branch, and averages the TMV of the BMA models at higher levels. The Z3D1L BMA model in Figure 6 shows the averaging of the IK variance of the three calibrated models Z3D1LExp, Z3D1LGus and Z3D1LPen. Regions with close proximity to the geophysical logs have lower variance values. This is expected since Kriging variance depends only on the distance from the observation points in which the variance of the estimation error is zero at the data location, and regions with less data have higher variance. The vertical strips of high uncertainty values of the Z3D1 model in Figure 6 illustrates that the WMV in the second level is based on the TMV of the first level. In addition, the WMV sub-plots of Z3 model and HBMA model in Figure 6, illustrate the previous remake that the WMV does not monotonically increase in value, yet more uncertainly regions are being added. This provides an important remark that the regions of uncertainty will always increase by adding more sources of uncertainty, but the variance values can decrease.

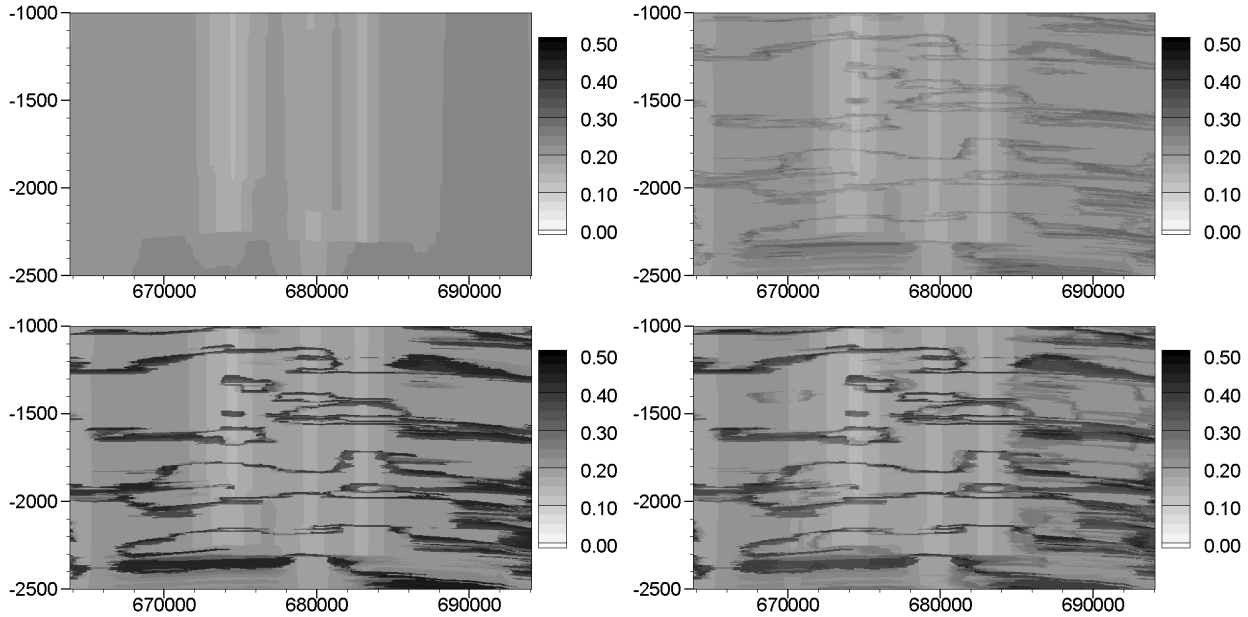

Figure 6. WMV at south side of DSS fault for BMA models Z3D1L, Z3D1, Z3 and HBMA.

The last part of the variance discussion is the TMV, which represents the total uncertainty. The first sub-plot of Figure 7 shows the TMV adds the BMV and WMV. The propagation of uncertainty and the monotonic adding up of uncertainty for the branch of the best model is clearly depicted in Figure 7. Another noticeable remake is that the BMV is taking over the WMV, which indicates that uncertainty due to different levels of uncertainty and competing propositions in each level is higher than the uncertainty arising from the different IK variances of the competing models.

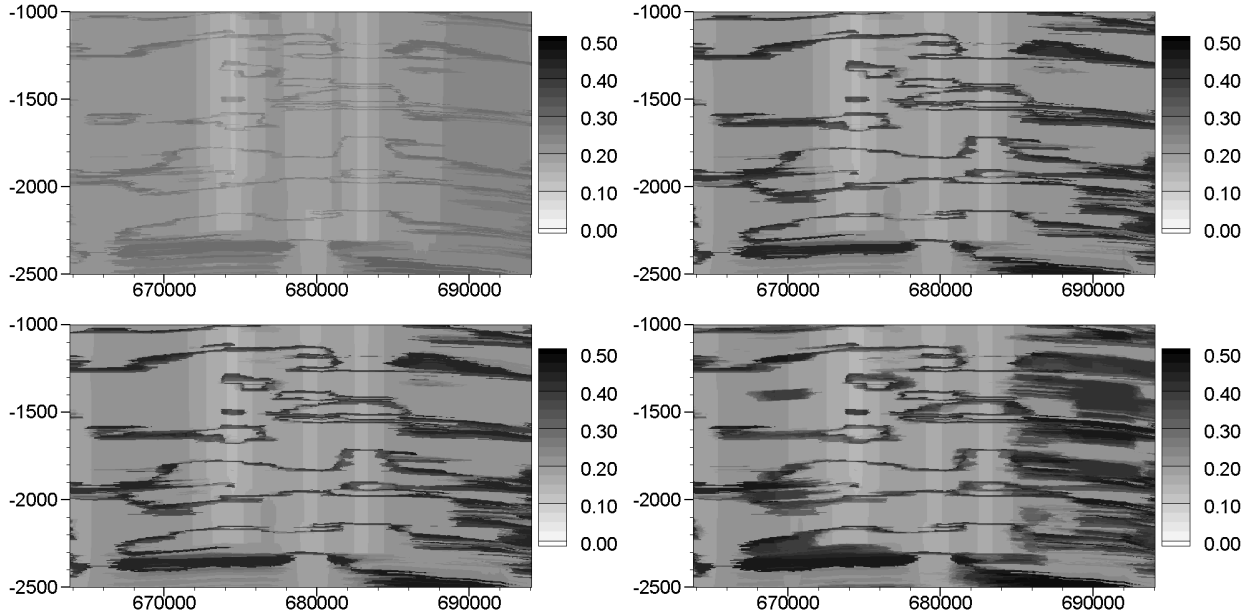

Figure 7. TMV at south side of DSS fault for BMA models Z3D1L, Z3D1, Z3 and HBMA.

Development of a 2D Hydrodynamic Model of the Mississippi River and Application To Long-Term Management Scenarios, Contaminant Transport and Sediment Transport

Basic Information

Title:	Development of a 2D Hydrodynamic Model of the Mississippi River and Application To Long-Term Management Scenarios, Contaminant Transport and Sediment Transport
Project Number:	2011LA79B
Start Date:	3/1/2011
End Date:	2/28/2012
Funding Source:	104B
Congressional District:	5th
Research Category:	Climate and Hydrologic Processes
Focus Category:	Hydrology, Sediments, Solute Transport
Descriptors:	None
Principal Investigators:	Clinton S. Willson, Clinton S. Willson

Publications

1. Willson, C.S. et al., 2012 Linking Science, Engineering and Design in Envisioning the Future of Coastal Louisiana: A Study of the Lowermost Mississippi River, to be presented at the 2012 State of the Coastal Conference being held in New Orleans, LA
2. Willson, C.S. et al., 2012, Envisioning a Sustainable Future for the Lower Mississippi River: Linking Engineering, Science and Design, to be presented at the CUAHSI 3rd Biennial Colloquium on Hydrologic Science and Engineering Science Sessions: July 16-18, 2012

SYNOPSIS

Title: Development of a 2D Hydrodynamic Model of the Mississippi River and Application To Long-Term Management Scenarios, Contaminant Transport and Sediment Transport

Project Number 2011LA79B

Start Date March 1, 2011

End Date February 28, 2012

Funding Source 104B

Research Category: Climate and Hydrologic Processes

Focus Categories Hydrology (HYDROL), Sediments (SED), Solute Transport (ST),

Descriptors Mississippi River Hydrodynamics, Fate-and-Transport, Sediment Transport

Primary PI Clinton S. Willson

Other PIs None

Problem and Research Objectives

The Mississippi River has an annual average flow rate of 495,000 cfs (ranks seventh worldwide in both annual sediment and water discharge) and drains approximately 1,245,025 mi^2 representing about 41% of the 48 contiguous United States (Knox, 2007) (NAP, 2008). The coastal system that the river created and the ease of passage to/from the Gulf of Mexico for ports up to Baton Rouge make the lower river of vital economic importance to Louisiana and the U.S. The availability of freshwater and ease of navigation has also provided for a large presence on the river of petrochemical plants and related industry. While not a regular occurrence, unintended releases of chemicals within and along the banks of the river occur and can have major consequences for drinking water supplies and ecological systems. Finally, there are a number of proposed projects that intend to utilize Mississippi River water and its resources (e.g., nutrients, sediment) for coastal and wetland restoration projects. Improved understanding of the hydrodynamics of the river and transport of these resources is crucial for optimal planning and utilization.

Here, we are developing two complimentary models of the Mississippi River from Tarbert Landing out into the Gulf of Mexico that can be used for three purposes: (1) simulate the river hydraulics under potential future scenarios associated with climate change or changes in river management; (2) model the fate-and-transport of chemicals downriver from any location within the study domain; and (3) model the sediment transport dynamics to better understand the timing and delivery of sediment to the lowermost reaches of the river. These models will be useful for state and federal agencies, public officials/decision-makers, researchers and consulting firms in making technically-sound decision regarding the river and its resources.

Methodology

We have already developed and calibrated a 1D HEC-RAS model of the river from Tarbert Landing to the Head of Passes. This 1D model was built using the latest bathymetry and topography data along the river and has been calibrated and validated for the 2009. This same bathymetry and topography is currently being used in our development and calibration of the 2D Adaptive Hydraulics (ADH) finite element model covering the same reach of the river.

Principal Findings and Significance

The HEC-RAS model has been used to model a number of scenarios, including: (1) the impact of both eustatic sea level rise and subsidence on the lower river hydraulics; (2) the impact of a major lower river realignment on the lower river hydraulics.

The Louisiana Coastal Protection and Restoration Authority has issued a draft report regarding Mississippi River Delta Plain future subidence and local eustatic sea level rise rates. The HEC-RAS model was run under various flow rates (low, medium and high) to look at the water surface elevations, velocities, and sediment transport characteristics for: (1) current conditions; (2) a scenario where the relative sea level rise (i.e,. due to both subsidence and eustatic sea level rise) is accounted for by simply raising the Gulf of Mexico +1 and +1.5 m; and (3) a scenario where the bathymetry and topography in the lower river is lowered to account for local subsidence rates and the Gulf of Mexico water level is raised to account for eustatic sea level rise.

Figure 1 shows the river velocity values for the three scenarios at a flow rate of 1,000,000 cfs while Figure 2 shows the bottom shear stress values for the same conditions. In both cases, it is clear that the combined effects of subsidence and sea level rise will cause the lower river to flatten out causing decreases in the velocity and in the sediment carrying capacity. These characteristics may create problems related to navigation and will likely increase the need to dredge more of the river. Figure 3 shows the water surface elevations from the HEC-RAS model for 2009 flow rates: simulated and observed for 2009 conditions; simulated for a river that is realigned to end around RM 55; and simulated for a river that is realigned to end around RM 30. By realigned, we mean that the river has been "shortened" around either River Mile (RM) 55 or 30 so that ~80% of the river is diverted to build land and ~ 20% flows through a relatively slackwater navigation channel. The results in Figure 3 first show the good quantitative match between the simulated and observed 2009 water surface elevations. Second, it is obvious that a shortened river will increase the hydraulic efficiency of the river and reduce water surface elevations in an above the New Orleans area. The bottom shear stress in the river at a flow rate of 1,000,000 cfs for current conditions and one of the river realignment scenarios is shown in Figure 4. While a realigned river may reduce water surface elevations, the changes will also impact water velocities, sediment transport, etc. Figure 4 also highlights how this modeling work is eventually going to integrate with

socioeconomic data and information being gathered by the LSU Coastal Sustainability Studio (www.css.lsu.edu); in the figure, the water surface elevation is shown along with population data. Note: These modeling results (particularly, the ones with the shortened/realigned river) are very preliminary and are included mostly to show the type of future management scenarios that we are looking to address with our model(s).

The 2D model is currently being calibrated and validated with initial results expected by the end of Summer 2012.

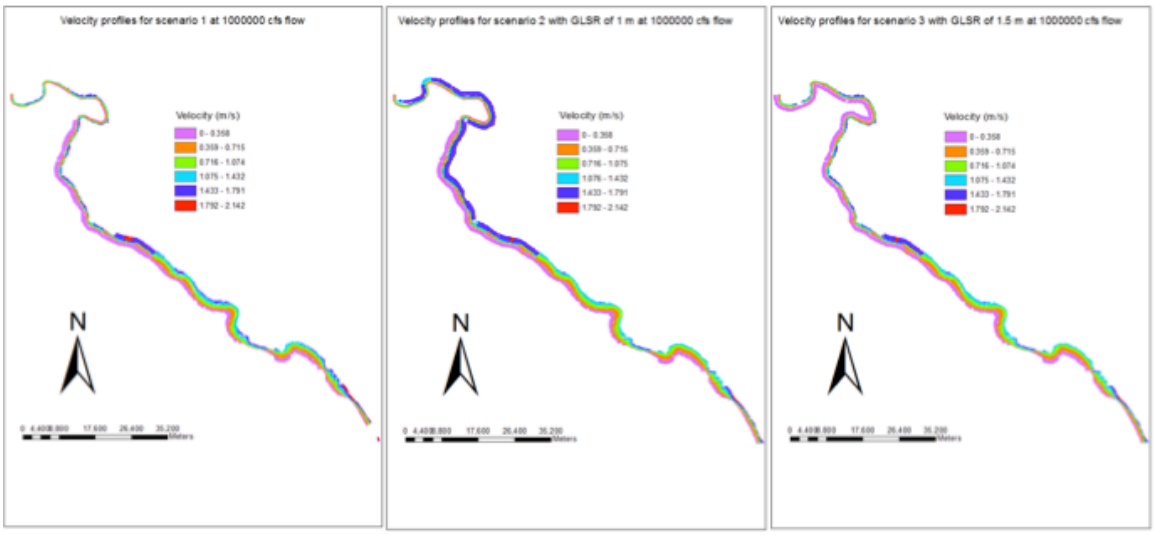

Figure 1: River velocity profiles for the lower ~110 miles of the Mississippi River at a flow rate of 1,000,000 cfs and three conditions (left: current; center: relative sea level rise of 1.5 m all accounted for through Gulf of Mexico; right: subidence and eustatic sea level rise accounted for independently.

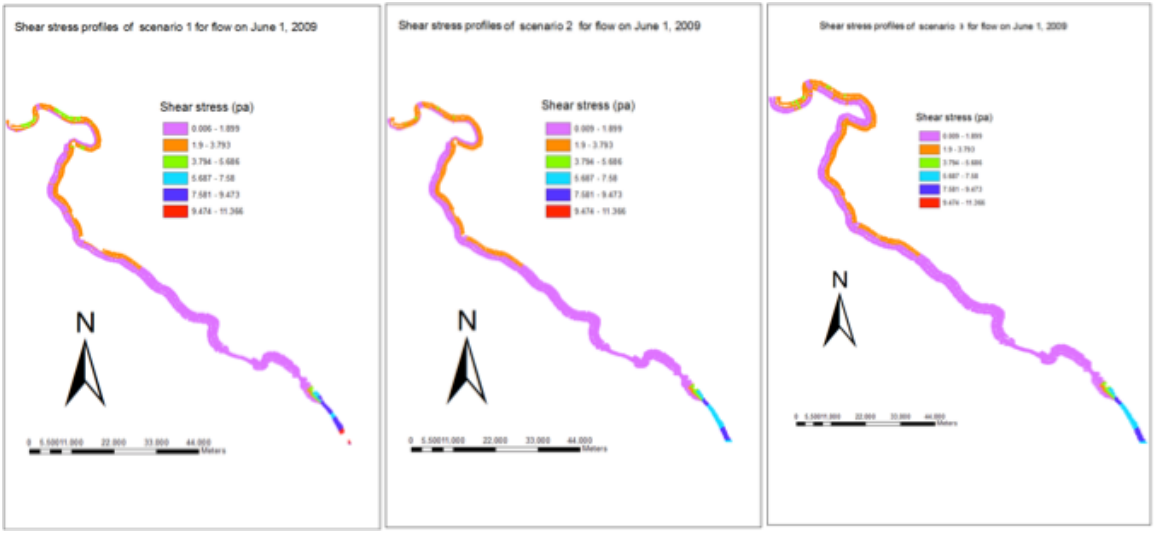

Figure 2: River shear stress profiles for the lower ~110 miles of the Mississippi River at a flow rate of 1,000,000 cfs and three conditions (left: current; center: relative sea level rise of 1.5 m all accounted for through Gulf of Mexico; right: subidence and eustatic sea level rise accounted for independently.

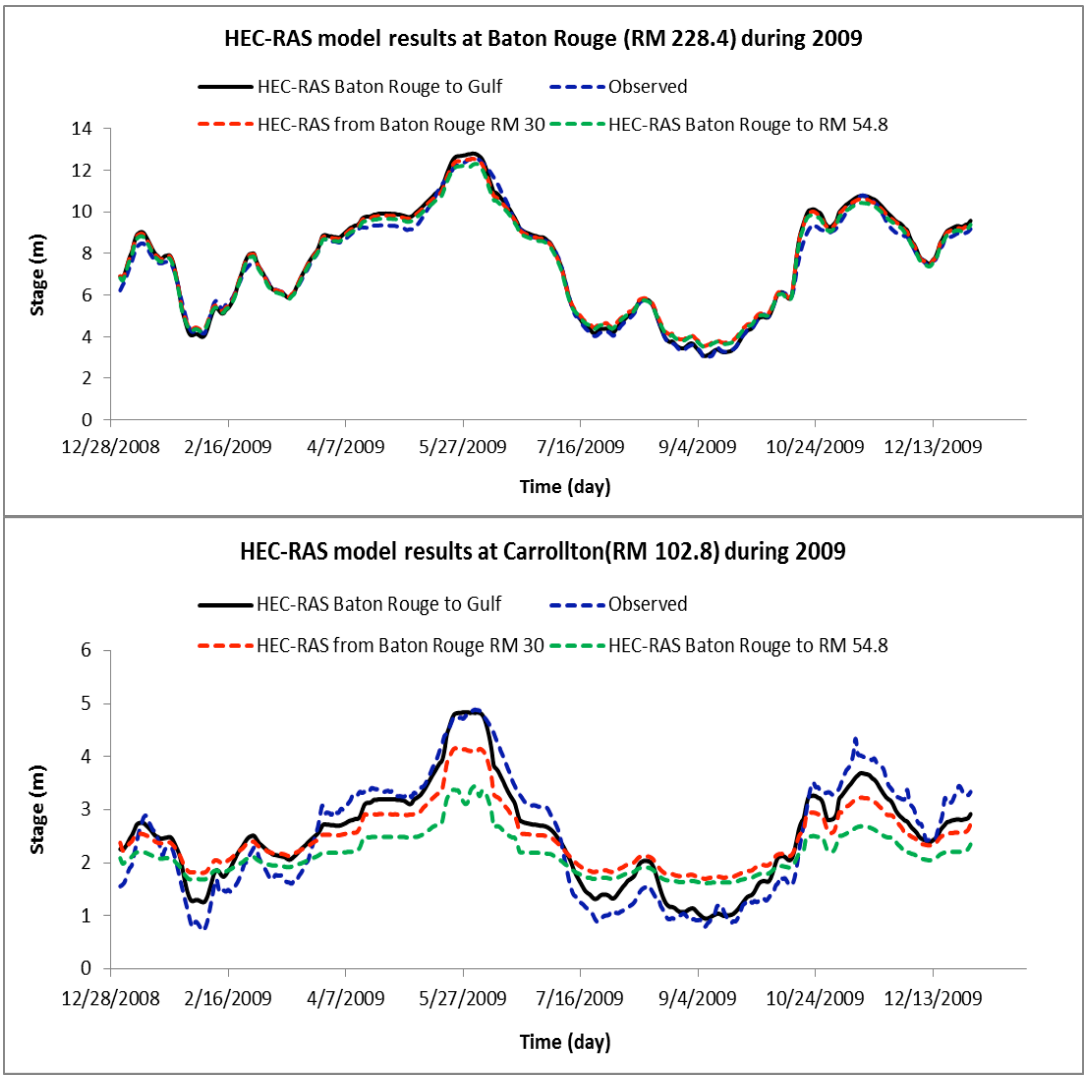

Figure 3: Water Surface Elevations for Baton Rouge (top) and Carrollton (bottom) during 2009 flow rates for simulated and observed 2009 conditions and for two shortened/realigned river scenarios.

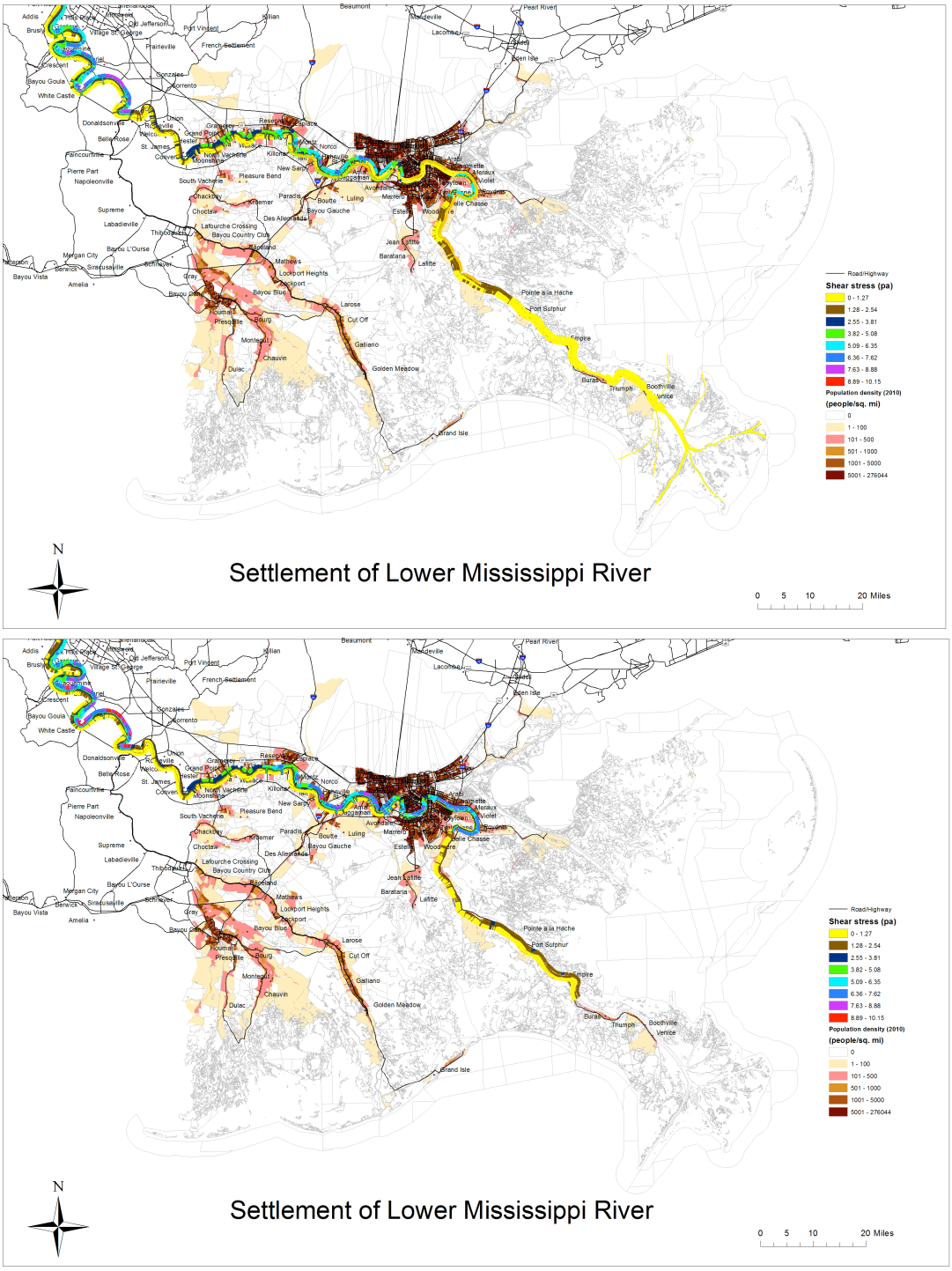

Figure 4: Bottom Shear Stress Values at a flow rate of 1,000,000 cfs for current conditions (top) and for a shortened/realigned river (bottom).

Feasibility Study of Scavenging Approach to Stop Saltwater Toward Water Wells

Basic Information

Title:	Feasibility Study of Scavenging Approach to Stop Saltwater Toward Water Wells
Project Number:	2011LA81B
Start Date:	3/1/2011
End Date:	2/28/2012
Funding Source:	104B
Congressional District:	6th
Research Category:	Ground-water Flow and Transport
Focus Category:	Groundwater, Solute Transport, Management and Planning
Descriptors:	None
Principal Investigators:	Frank Tsai

Publications

1. Frank Tsai, 2011, Multimodel Uncertainty Analysis for Chance-Constrained Saltwater Intrusion Management, Louisiana Water Resources Research Institute, Louisiana State University, Baton Rouge, Louisiana, 10 pages. (USGS 104B)
2. Tsai, F. T.-C., and A.S. Elshall. (2011). A Hierarchical Bayesian Model Averaging Approach to Cope With Sources of Uncertainty in Conceptual Ground Water Models, World Water & Environmental Resources Congress, Palm Springs, CA, May 22-26, 2011.
3. Tsai, F. T.-C. (2011). Development of Scavenger Well Operation Model To Stop Saltwater Intrusion Toward Water Wells In The “1,500-Foot” Sand of The Baton Rouge Area, Louisiana, World Water & Environmental Resources Congress, Palm Springs, CA, May 22-26, 2011.
4. Tsai, F. T.-C. (2011). Scavenger Wells Stop Saltwater Intrusion in Baton Rouge, Louisiana, MODFLOW and More 2011, Golden, CO, June 5-8, 2011
5. Elshall, A. S., F. T.-C. Tsai, and J. S. Hanor. (2011). Uncertainty and Characterization of the Baton Rouge Fault System in a Bayesian Framework, 2011 American Geophyiscal Union Fall Meeting, December 5-9, 2011, San Francisco, CA.
6. Chitsazan, N., and F. T.-C. Tsai. (2011). A Chance-Constrained Multimodel Approach to Design a Saltwater Intrusion Mitigation Plan, 2011 American Geophysical Union Fall Meeting, December 5-9, 2011, San Francisco, CA.
7. Hanor, J. S., E. L., Chamberlain, and F. T.-C. Tsai. (2011). Evolution of the Permeability Architecture of the Baton Rouge Fault Zone, Louisiana Gulf Coastal Plain, 2011 American Geophyiscal Union Fall Meeting, December 5-9, 2011, San Francisco, CA.

SYNOPSIS

Title: Feasibility Study of Scavenging Approach to Stop Saltwater Toward Water Wells
Project Number:
Start Date: 3/1/2011
End Date: 2/29/2012
Funding Source: 104B
Congressional District: Louisiana
Research Category: Ground-water Flow and Transport
Focus Category: Ground Water, Solute Transport, Management & Planning
Descriptors: Prediction, Remediation, Saltwater Intrusion, Aquifer, Subsurface, Modeling, Optimization, Management
Primary PI: Frank T.-C. Tsai

Problem and Research Objectives

Due to excessive groundwater withdrawal, many Louisiana freshwater aquifers are being contaminated by saltwater intrusion. The major aquifer systems affected include the Chicot aquifer system of southwestern Louisiana, the Sparta aquifer system of northern Louisiana, and the Southern Hills aquifer system in the Baton Rouge Capital Area.

The project focuses on saltwater intrusion mitigation in the Southern Hills aquifer system in the Baton Rouge area. The aquifer system consists of a sequence of aquifers and aquicludes, which extends to a depth of about 3,000 feet. Prior to heavy pumping, freshwater was effectively isolated from saltwater to the south by the low permeable Baton Rouge fault. Recent USGS monitoring wells (EB-917 and EB-918 for the "1,500-foot" sand, EB-630, EB-1028, and EB-1150 for the "2,000-foot" sand), reveal progressive saltwater intrusion toward public and industrial water wells in the "1,500-foot" sand and "2,000-foot" sand (Lovelace, 2009). Water wells may be forced to reduce withdrawal rates or cease pumping altogether if saltwater encroachment cannot be stopped. Insufficient groundwater will critically hamper economic development in the Capital Area.

The goal of the project is to develop a scavenger well operation (SWOP) model to halt saltwater movement in the "1,500-foot" sand toward the water wells at Lula pump station operated by the Baton Rouge Water Company. The study area is shown in Figure 1. On October 28, 2009, chloride concentration of 182 mg/L was measured at the water well EB-658 (Lula-19). This poses a concern that a high chloride front may have come near the Lula wells. To better understand the current situation of saltwater intrusion and to resolve this urgent issue, the SWOP model aims to utilize scavenger wells to prevent high chloride concentration from reaching Lula wells. Scavenger wells are small extraction wells to be placed at a certain distance in front of water wells to capture and intercept saltwater. The decision variables in the SWOP model are the number, location, and extraction rate of scavenger wells.

Specific objectives are to:
(1) Understand the past, current, and future saltwater intrusion patterns
(2) Estimate the flux of groundwater flow across the Baton Rouge fault
(3) Estimate the flux of chloride concentration across the Baton Rouge fault

(4) Determine the number, location, and extraction rate of scavenger wells that can effectively stop saltwater intrusion to EB-658
(5) Evaluate the impact of scavenger wells on increasing saltwater intrusion across the fault

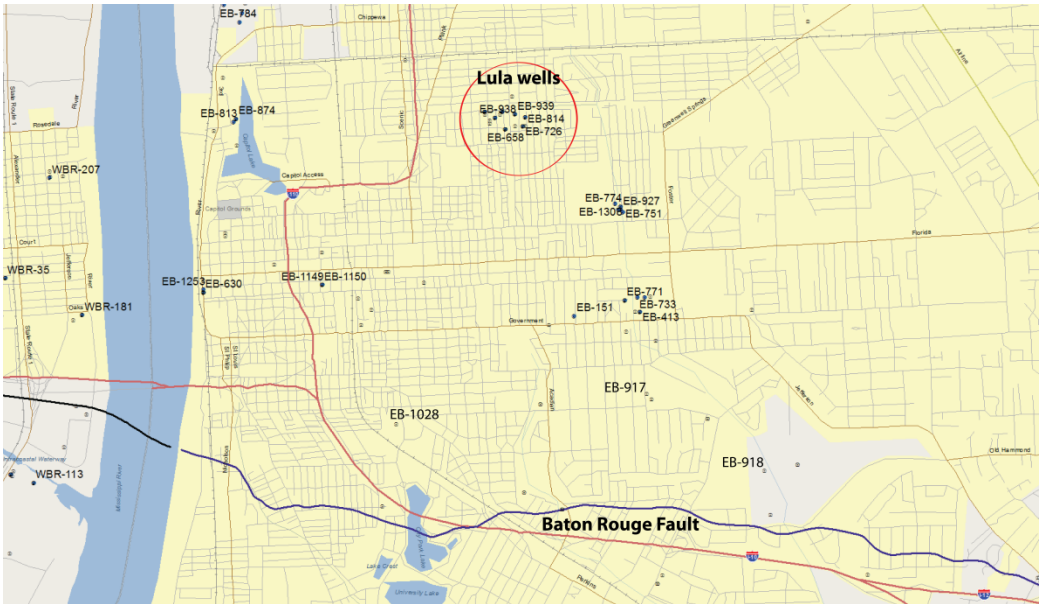

Figure 1: Study area. The base map is created by Louisiana GIS Digital Map 2007. The Baton Rouge Fault line is obtained from McCulloh and Heinrich (2012).

Methodology - Saltwater intrusion model development and calibration

The entire modeling period was divided into a model calibration period and a model prediction period. Model calibration period was from 1/1/1945 to 12/31/2009, a 65-year period. In the calibration period, groundwater head data and chloride data were used to estimate model parameters. Simulated groundwater head and chloride concentration distributions at the end of 12/31/2009 were used as initial conditions (beginning of 1/1/2010) for the model prediction period. Model prediction period was a 50-year period from 1/1/2010 to 12/31/2059. Twelve (12) scenarios of scavenger well operations were tested in the model prediction period.

In the report, modeling results at the beginnings of three specific dates (1/1/2010, 1/1/2035, and 1/1/2060) were particularly discussed. These three dates served as the check points to evaluate groundwater heads and chloride concentrations at the current situation and situations after 25 and 50 years. It is noted that the information at the beginning of 1/1/2010 was that at the end of 12/31/2009, the information at the beginning of 1/1/2035 was that at the end of 12/31/2034, and the information at the beginning of 1/1/2060 was that at the end of 12/31/2059.

The "1,500-foot" sand saltwater intrusion model was developed using MODFLOW (Harbaugh et al., 2000) and MT3DMS (Zheng and Wang, 1999) under Groundwater Modeling System (GMS) (AQUAVEO^{TM}). The terrain of the study area covers the Baton Rouge metropolitan area. The eastern boundary of the study area extended to the Amite River, the western boundary was along the Mississippi River, the northern boundary intersected the north end of I-110 freeway, and the southern boundary was around 600 meters south of the Baton Rouge fault. It covered an area of around 300 km^2. The area was discretized into 188 rows, 195 columns, and 1 layer. Coarse

computational cells of 200 m by 200 m were given at the northeastern area, where saltwater intrusion was not a concern. Finer computational cells of around 50 m by 50 m were given to the area of ongoing saltwater intrusion. The aquifer thickness was determined from the prior studies (Tsai and Li, 2008; Li and Tsai, 2009).

It was understood that saltwater intrusion is a density-dependent flow process. Flow process should be coupled with mass transport process at each time step to reveal encroachment of denser saltwater near the bottom of an aquifer. Since this modeling study served for the planning purpose and only considered one vertical layer to the "1,500-foot" sand in order to reduce computation complexity, density effect was not simulated. This means that MODFLOW and MT3DMS were decoupled. MODFLOW was run first to obtain groundwater levels. Then, MT3DMS was run using MODFLOW solutions to simulate intrusion of chloride concentration. In the future work, density effect can be simulated by discretizing the aquifer thickness into multiple layers.

In order to better predict the history of saltwater intrusion in the "1,500-foot" sand, the starting date of modeling was 1/1/1945. This was determined according to the timeline of installation of the BRWC water wells in the "1,500-foot" sand. The first BRWC water well EB-413 was installed in 1946 at the Government pump station. From USGS studies (Meyer and Turcan, 1955), saltwater intrusion in the study area was not reported prior to 1946. In this study, the period prior to 1946 is denoted as the pre-anthropogenic pumping period. Detailed initial groundwater head and chloride concentration at 1/1/1945 and boundary condition from 1/1/1945 to 12/31/2009 were given in Tsai (2011)

(1) Water wells

Sixteen (16) water wells were installed in the study area during the period 1/1/1945-12/31/2009. Pumpage data was obtained from the Capital Area Ground Water Conservation Commission (CAGWCC) and BRWC. EB-504 was a BRWC water well, which was completed in 1949 and was out of service in 1979. EB-1295C (Stumberg-02) screened both the "1,500-foot" and "1,700-foot" sands. CAGWCC assigned EB-1295C pumpage record to the "1,500-foot" sand. This study included EB-1295C water well.

There was no pumpage data for EB-371B and EB-773 prior to 1975. EB-371B was completed in 1941 (Meyer and Turcan, 1955). Monthly pumpages for 1945-1974 at EB-371B and for 1964-1974 at EB-773 were determined by their 5-year monthly pumpage averages (1975-1979).

BRWC had lump sum pumpage data at water wells EB-413 and EB-504 for 1953-1962. To split EB-413 from EB-504 for this period, weighting coefficients for EB-413 were determined using the ratios of three-year monthly pumpage averages (1975-1977) to lump sum pumpages: EB-413 pumpages/(EB-413+EB-504 pumpages). BRWC also had lump sum pumpage data of water wells EB-413, EB-504, and EB-771 for 1963-1974. The same approach of deriving weighting coefficients was applied to splitting the lump sum pumpages for this period.

BRWC had lump sum pumpage data of water wells EB-510, EB-657, EB-658, EB-726, EB-938, and EB-939 for 1953-1974. For splitting the pumpages, weighting coefficients were obtained

using the ratios of five-year monthly averages (1975-1979) of their individual pumpages to the lump sum pumpages in this 5-year period.

Finally, the monthly pumpages for 1946-1952 at EB-413 were determined by 5-year monthly pumpage averages (1953-1957). The monthly pumpages for 1949-1952 at EB-504 were determined by 5-year monthly pumpage averages (1953-1957).

(2) The "Connector" Well

The connector well, EB-1293, started in April 1999. Since the recorded groundwater data at EB-1293 did not represent head in the "1,500-foot" sand, the head data could not be used to assign a constant head boundary condition, or could not be used to compare to simulated water levels at EB-1293. Instead, recorded flow rate was used to represent EB-1293 as an injection well in the model. According to January 2009 CAGWCC Newsletter, the average injection rate was 475 gallons per minute or 2,589 m^3/day (or 0.684 mgd).

Principal Findings and Significance

(1) Saltwater intrusion analysis for 1/1/1945-12/31/2009

Homogeneous hydraulic conductivity of 55 m/day was used in the groundwater model. A homogeneous fault hydraulic characteristic (fault hydraulic conductivity per unit fault width) (Hsieh and Freckleton, 1993) was estimated 8.0×10^{-4} day^{-1} for a segment from the west boundary to the intersection of Wards Creek and Corporate Boulevard. The other segment of the fault had a relatively low hydraulic characteristic value of 3.5×10^{-4} day^{-1}. Although not shown here due to page limit, simulated groundwater levels compare well to the observed data for different time periods at several USGS observation wells. According to water level in EB-917, groundwater level declined at a rate of 1.31 m/year (4.3 ft/year) before 1980, 0.40 m/year (1.3 ft/year) in the 1980s and 1990s, and 1.16 m/year (3.8 ft/year) after 2000. According to the simulated groundwater head distribution, a cone of depression centered at Lula pump station is evident.

Pore water pressure differences and groundwater flow velocity (Darcy velocity) across the Baton Rouge fault were estimated at a single point using simulated groundwater heads at EB-782B and at its adjacent computational cell (134, 71) south of the fault. Using the harmonic mean approach, equivalent hydraulic conductivity for this calculation was obtained 0.081 m/day. The results are shown in Figure 2. Negative water pressure difference and negative flow velocity occurred at the beginning of a few years of simulation because of southward flow across the fault. Figure 2 shows a trend of increasing pressure difference and flow velocity in the last 10 years (2000-2009). Pressure difference on 1/1/2010 was estimated at 43 psi (pounds per square inch). The flow velocity was estimated at 4.84×10^{-2} m/day on 1/1/2010.

The maximum head pressure difference on 1/1/2010 occurred around 100 m west of the intersection of Dalrymple Drive and the fault line. The computational cell (137, 39) south of the fault had groundwater head of -7.957 m and the computational cell (136, 39) north of the fault had groundwater head -38.852 m. This resulted in head difference 44 psi and flow velocity m/day on 1/1/2010. The maximum pressure difference was only one psi higher than that at EB-782B.

Porosity was estimated 27%, longitudinal dispersivity was estimated 180 m, and transverse dispersivity was estimated 0.36 m. The same homogeneous porosity, longitudinal dispersivity, and transverse dispersivity were used for both "1,200-foot" sand and "1,500-foot" sand. It was observed that major chloride concentration at EB-917 and EB-918 might be the result of lateral-flow-driven chloride transport along the fault from the east side. Therefore, a high ratio of longitudinal dispersivity to transverse dispersivity was obtained to reveal faster chloride transport to EB-807A and EB-658, but slower chloride transport to EB-917 and EB-918.

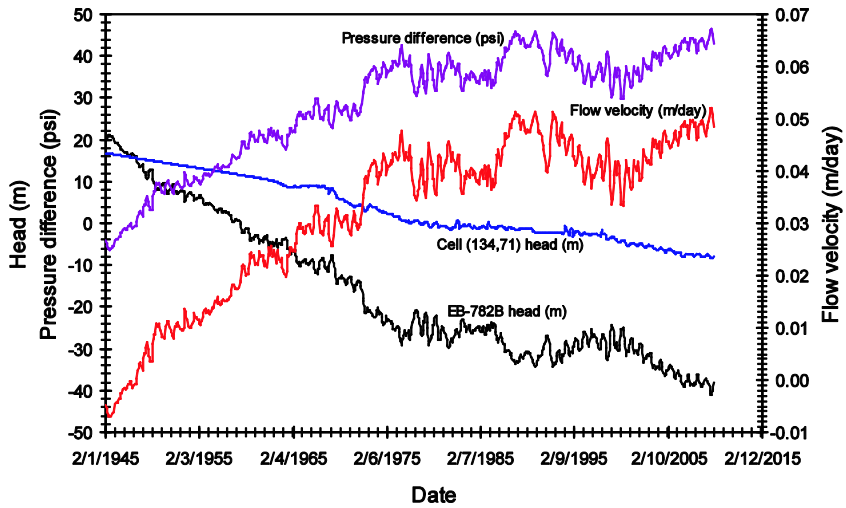

Figure 2: Simulated groundwater heads at EB-782B and at its adjacent computational cell (134, 71) south of the fault, pressure difference (psi), and flow velocity (m/day).

Simulated chloride breakthroughs were compared to chloride data. Simulated chloride concentrations showed up earlier compared to lower chloride data at EB-807A, but were similar to high chloride data. Simulated chloride concentrations showed good agreement to the chloride data at EB-807A after 1981, and to the chloride data at EB-917 and EB-658 after 2000. Simulated chloride concentrations were underestimated at EB-918 after 2000. This indicates that chloride transport simulation along the fault from the eastern side needs more study. However, the lateral-flow-driven chloride concentration showed less impact on EB-658 and EB-807A.

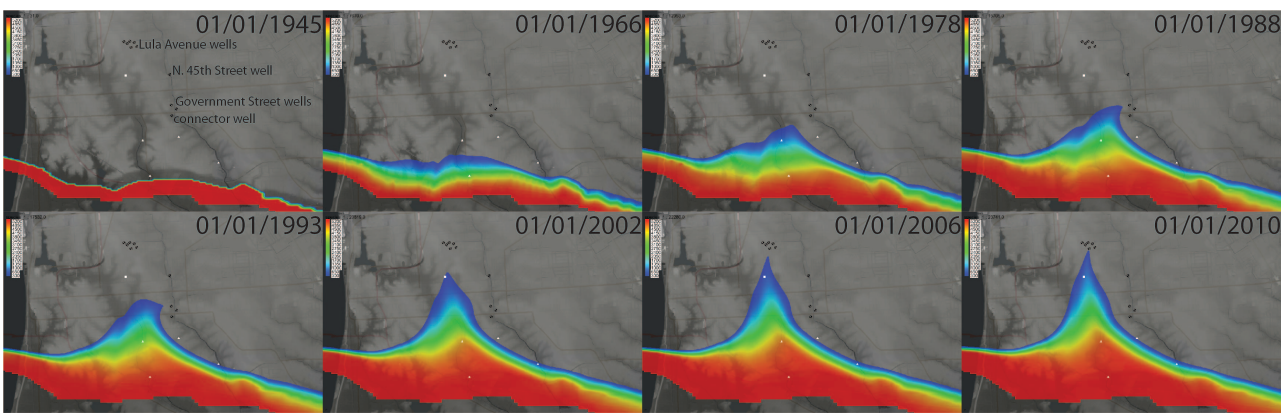

Figure 3: Saltwater intrusion pattern. Front line represents chloride concentration of 250 mg/L.

The 65-year simulation in Figure 3 shows a unique movement of the saltwater intrusion front. From 1945 to 1987, a single chloride front was developed and moved toward EB-771 (Government-06). From 1987 to 2001, the front started to retreat and a new front started to develop and move toward the Lula wells. From 2001 to 2009, a single front moved toward EB-658 (Lula-19). This unique movement of chloride concentrations was revealed by the "up-down-

up" chloride data at EB-917. The unique intrusion pattern is the combined effect of the low permeable Baton Rouge fault and dynamic anthropogenic pumping.

Chloride mass flux was estimated at a single point using simulated groundwater flow velocity simulated chloride concentrations at EB-782B and its adjacent computational cell (134, 71) south of the fault. The magnitudes of advective mass flux and dispersive mass flux were similar prior to 1957. After 1957, advective mass flux dominated dispersive mass flux due to high groundwater flow velocity. Dispersive mass flux was strong in 1955-1980. The total mass flux on 1/1/2010 was estimated 0.98 kg/day-m^2.

(2) Saltwater intrusion prediction-"No-action" scenario (no scavenger wells)

The saltwater intrusion model was run for 50 years from 1/1/2010 to 12/31/2059 without scavenger wells. Predicted breakthrough curves in EB-658 and other observation wells were used as baseline information to evaluate the stopping efficiency of various scenarios through using scavenger wells as presented in the following section.

To extend the saltwater intrusion model to predict chloride concentrations in the period 1/1/2010-12/31/2059, time-varied boundary values of groundwater head were estimated using the linear trend of head declination in the last 5 years, 1/1/2005-12/31/2009. The monthly pumpages of water wells were estimated based on 5-year (2005-2009) averaged pumpages. The total withdrawal rate at Government pump station (two water wells) was 2.53 mgd, at Lula pump station (six water wells) was 7.07 mgd, and at N. 45th pump station (one water well) was 1.69 mgd. The total pumpage of water wells was 12.45 mgd. The injection rate of the connector well remains 0.684 mgd, and chloride concentration at the southern boundary remains 5,500 mg/L throughout the prediction period.

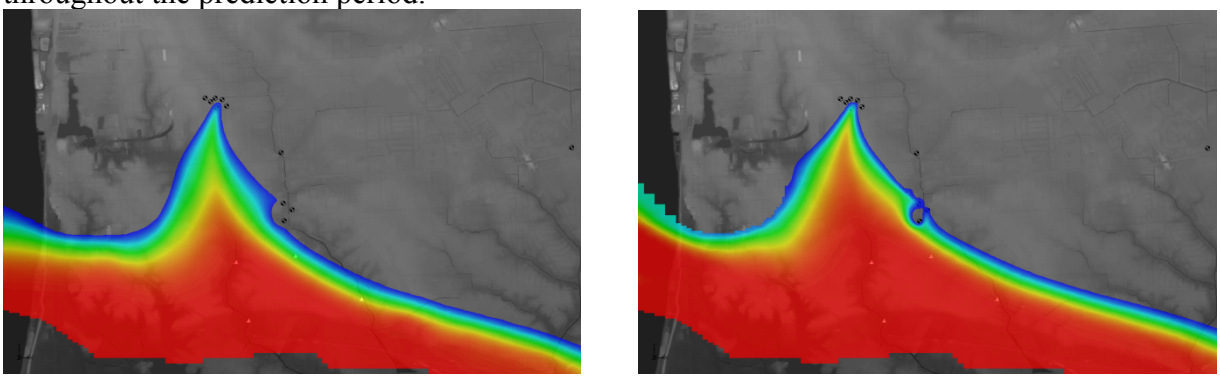

(a) 1/1/2035 (b) 1/1/2060

Figure 4: Chloride concentration distribution on (a) 1/1/2035, and (b) 1/1/2060 for the no-action scenario. The front line is 250 mg/L.

Chloride concentrations increase at EB-658, EB-807A, EB-917, and EB-918 in the period 1/1/1945-12/31/2059. Chloride concentration in EB-658 was predicted to 754 mg/L on 1/1/2035 and 1,540 mg/L on 1/1/2060. Figure 4 shows the concentration distributions on 1/1/2035 and 1/1/2060. Chloride concentrations in EB-807A, EB-917, and EB-918 were predicted to be thousands mg/L on 1/1/2035 and almost reach the maximum concentration 5,500 mg/L on 1/1/2060. Chloride concentrations in EB-413, EB-771, and EB-1293 were predicted tens mg/L on 1/1/2035, but would reach hundreds mg/L on 1/1/2060. Estimated chloride concentrations at N. 45th well, EB-927, were very low throughout the prediction period.

(3) Scenarios of stopping saltwater intrusion to EB-658 using scavenger wells

Twelve (12) scenarios listed in Table 1 were designed to reduce chloride concentration at EB-658. The starting date of using scavenger wells was assigned to 1/1/2011. The first four scenarios used one scavenger well with a constant extraction rate throughout the prediction period 1/1/2010-12/31/2059. Extraction rates with a 0.25 mgd (million gallons per day) increment increase were tested from 0.25 mgd to 1.00 mgd in scenario 1 to scenario 4, respectively. Scenarios 5-7 and scenario 9 used two concurrent scavenger wells, scenario 8 used three concurrent scavenger wells, and scenario 10 used four concurrent scavenger wells. Concurrent scavenger wells mean that scavenger wells were active from the beginning to the end of the prediction period. Scenarios 11 and 12 considered two sequential scavenger wells. The first scavenger well was active with an extraction rate of 0.50 mgd entirely throughout the prediction period. However, the second scavenger well was only active between 1/1/2036 and 12/31/2059.

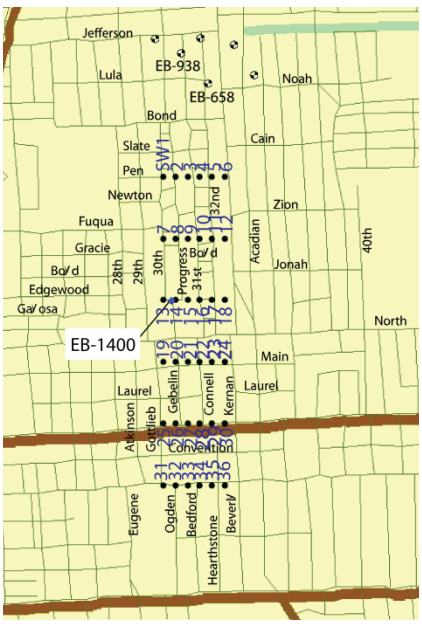

Figure 5: 36 potential locations of scavenger wells.

Table 1: Simulated chloride concentrations at EB-658 using the best solutions in individual scenarios.

Scenario	Scavenger well	Concentration (mg/L) 1/1/2035	1/1/2060
No action	-	754	1540
1	SW21 (0.25 mgd)	385	903
2	SW20 (0.50 mgd)	143	412
3	SW20 (0.75 mgd)	40	122
4	SW13 (1.00 mgd)	10	17
5	SW21, SW19 (2×0.25 mgd)	147	399
6	SW21, SW13 (0.25 mgd and 0.50 mgd)	35	114
7	SW20, SW19 (0.50 mgd and 0.25 mgd)	39	115
8	SW21, SW19, SW13 (3×0.25 mgd)	33	110
9	SW20, SW13 (2×0.50 mgd)	9	15
10	SW21, SW19, SW13, SW7 (4×0.25 mgd)	7	16
11	SW20, SW13 (0.50 mgd and 0.25 mgd)	143	116
12	SW20, SW13 (0.50 mgd and 0.50 mgd)	143	19

A total of 36 potential locations of scavenger wells, named from SW1 to SW36, were predetermined in Figure 5. The best locations of scavenger wells in the searching order and the simulated chloride concentrations in EB-658 on 1/1/2035 and 1/1/2060 are listed in Table 1. Scenarios 1, 2 and 5 are not feasible solutions for the period 1/1/2036-1/1/2060. Scenarios 6-12 were all feasible solutions to keep low chloride concentrations at EB-658 throughout the entire prediction period. We found that

(1) If scavenger wells were placed too close to the Lula wells, high chloride concentration would be dragged near the Lula wells. EB-658 would pump high chloride concentration in later time.

(2) If scavenger wells were placed far away from the Lula wells in a high chloride concentration zone, high chloride concentrations north of the scavenger well could not be caught. High chloride concentrations would eventually arrive at EB-658.

(3) Scavenger wells had a tendency to locate at the first three columns since the chloride concentration was slowly leaning to the west due to the impermeable zone at the west side.

(4) Using high extraction rate, there were many feasible locations to install scavenger wells, in addition to the best location. Scavenger wells at the best location give the lowest concentration at EB-658.

As shown in Figure 6, it was found that breakthrough curves at EB-658 using one single scavenger well and using multiple scavenger wells were similar for the same total extraction rates. For example, scenarios 3, 6, 7, and 8 used a total of 0.75 mgd, but different numbers of scavenger wells. The breakthrough curves were similar. Scenarios 4, 9, and 10 used a total of 1.00 mgd, but different numbers of scavenger wells. The breakthrough curves were similar. This result provides many options with the same total extraction rates.

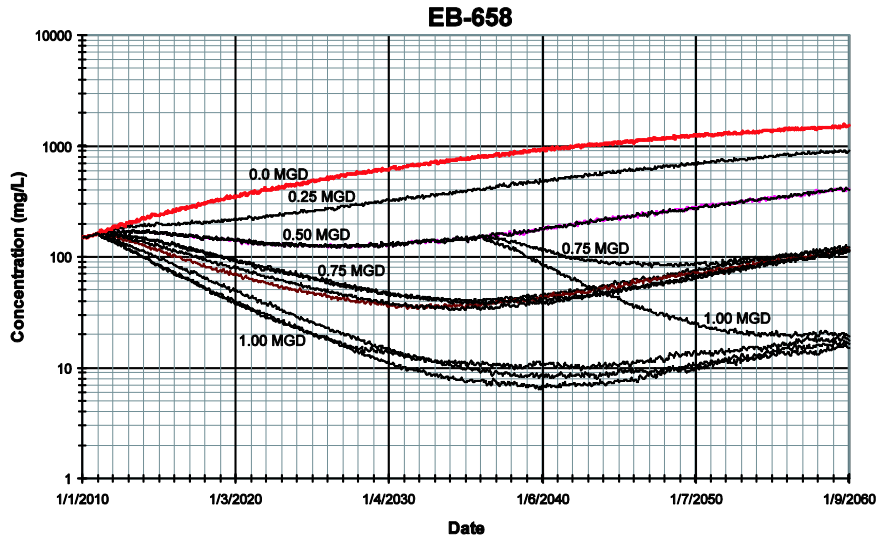

Figure 6: Predicted chloride concentration at EB-658 under different scenarios.

The impact of scenario 10 on the groundwater flow across the fault at EB-782B is not significant comparing to the current condition. Without scavengers, the pressure difference linearly increased from 43 psi on 1/1/2010 to 82 psi on 1/1/2060. The groundwater flow linearly increased from 4.84×10^{-2} m/ day on 1/1/2010 to 9.19×10^{-2} m/day on 1/1/2060. The total mass flux increased from 0.98 kg/day-m^2 on 1/1/2010 to 1.87 kg/day-m^2 on 1/1/2060. Those values showed a 90% increase in 2060 with respect to the values on 1/1/2010.

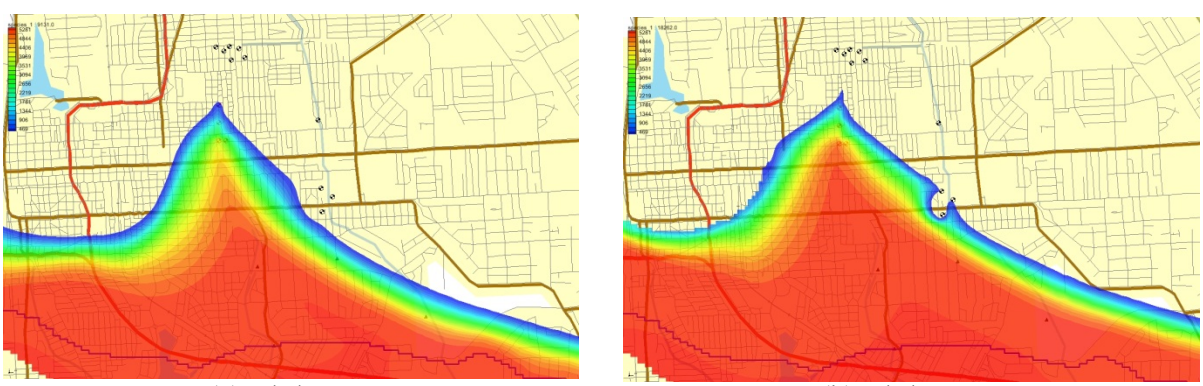

(a) 1/1/2035 (b) 1/1/2060

Figure 7: Chloride concentration distribution on (a) 1/1/2035 and (b) 1/1/2060 under scenario 10 (4 scavenger wells). The front line is 250 mg/L.

As shown in Figure 7, scenario 10 keeps the 250 mg/L front line away from the Lula wells for the next 50 years. However, the water wells at Government pump station would encounter high chloride concentration in 50 years. Using scenario 10, a total of one-mgd extraction rate caused

additional drawdown of 0.02 m south of the fault and additional drawdown of 1.66 m north of the fault compared to the no-action scenario. This resulted in an additional 2.33 psi pressure difference and 2.62×10^{-3} m/day groundwater flow velocity. The total mass flux increased by 0.051 kg/day-m^2. Those values counted for less than 6% increase with respect to the values on 1/1/2010.

Scenarios with 1 mgd extraction rate indicate that SW13 (UTM-NAD83 X=676779 m, Y=3370623 m) at Progress Park is the best location for installing a scavenger well. A new observation well, EB-1400 (N 30' 27.285, W 91' 09.509) at Progress Park between SW13 and SW14 was completed in 2011 by Layne. It can be converted to a scavenger well if permitted.

Three scenarios using 1-mgd interceptor wells (scavenger wells) were suggested by Layne Hydro (Layne Hydro 2012). Using the current model, Figure 8 shows that scenario 4 (one scavenger well at Progress Park) from this study outperforms Layne's three scenarios. This is because the location of scavenger wells was optimized in this study.

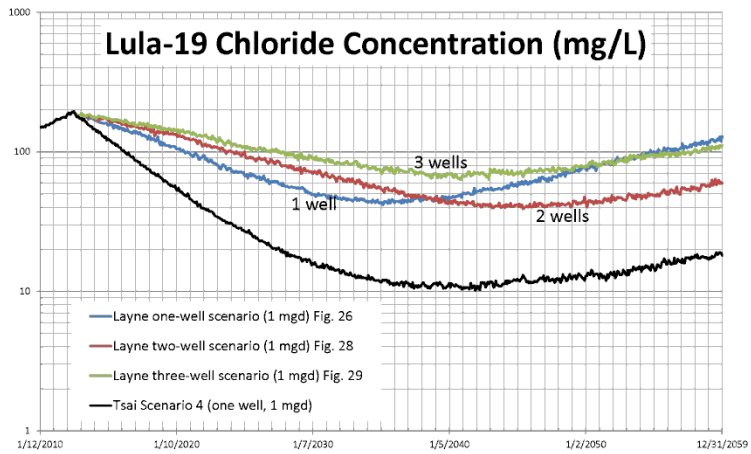

Figure 8: Comparison of scenario 4 with Layne's three scenarios.

References

Harbaugh, A. W., E. R. Banta, M. C. Hill, and M. G. McDonald. (2000). MODFLOW-2000, the U.S. Geological Survey modular ground-water model: User guide to modularization concepts and the ground-water flow process. U.S. Geological Survey Open-File Report 00-92.

Layne Hydro (2012). Remedial Options for Saltwater Encroachment in the 1,500-Foot Sand, prepared for Baton Rouge Water Company

Lovelace, J.K. (2009). Ground Water Levels and Salt Water Encroachment in Major Aquifers in Louisiana, USGS, presentation in USEPA 2009 Ground Water Summit, February 4, 2009.

McCulloh, R. P., and P. V. Heinrich. (2012) Surface Faults of the South Louisiana Growth-Fault Province, *in* Cox, R. T., M. Tuttle, O. Boyd, and J. Locat, eds., Recent Advances in North American Paleoseismology and Neotectonics east of the Rockies and Use of the Data in Risk Assessment and Policy, Geological Society of America.

Meyer, R. R., and A. N. Turcan, Jr. (1955). Geology and Ground Water Resources of the Baton Rouge Area, Louisiana, Louisiana: U. S. Geological Survey Water-Supply Paper 1296, 138p

Tsai, F. T.-C. (2011). Scavenger Well Operation Model to Assist BRWC to Identify Cost-Effective Approaches to Stop Saltwater Intrusion towards the BRWC Wells in the "1,500-Foot" Sand of the Baton Rouge Area. Prepared for Baton Rouge Water Company and Capital Area Ground Water Conservation Commission.

Zheng, C., and P. Wang. (1999). MT3DMS, A modular three-dimensional multispecies transport model for simulation of advection, dispersion and chemical reactions of contaminants in groundwater systems (Release DoD_3.50.A), Documentation and User's Guide.

- ll 2010)

Turbulent Interactions of Coastal Vegetation and Waves

Basic Information

Title:	Turbulent Interactions of Coastal Vegetation and Waves
Project Number:	2011LA82B
Start Date:	3/1/2011
End Date:	2/28/2012
Funding Source:	104B
Congressional District:	6th
Research Category:	Climate and Hydrologic Processes
Focus Category:	Sediments, Wetlands, Geomorphological Processes
Descriptors:	None
Principal Investigators:	Heather Smith

Publications

There are no publications.

Project Title: Turbulent Interactions of Coastal Vegetation and Waves
Project Number: Research
Start Date: March 1, 2011
End Date: February 28, 2012
Funding Source: 104B
Congressional District: 6
Research Category: Coastal Engineering - Water Resources
Focus Categories: Waves, vegetation, wetlands, turbulence
Principal Investigator: Heather D. Smith

Problem Description

Critical Regional or State Water Problems

The deltaic coast of Louisiana is a unique environment. The formation of the delta through sediment deposition from the Mississippi River formed large coastal plains over thousands of years. However, within the last hundred years, anthropogenic changes to the river system to help reduce the impact of yearly floods have severely impacted the Mississippi River Delta system. The most important of which is the restriction of the river's natural pathway change through the construction levees, which cuts the wetlands of the deltaic plains off from the sediment supplied by the river. The decrease in sediment supply in the river has contributed to the decay of the natural ability of the coastline to reduce the impact of storms in the Gulf of Mexico through the loss of both barrier islands and wetlands. Wetlands are of particular interest, as they serve many functions including providing habitat for animals, trapping sediment from the water column and stabilizing the deposition through root production, and reducing the impact of storm surge and waves. It is estimated that roughly 4900 km^2 of wetlands in coastal Louisiana have been lost due to a combination of wave erosion at wetland edges and a sediment supply rate that is lower than the rate of subsidence. However, the ability to estimate the amount of wave reduction through natural coastal vegetation is severely limited, due to a lack of available data to elucidate the complex physics involved with the wave-vegetation interaction.

The modeling efforts to simulate the reduction of wave height have considered two approaches. The first, which is popular in depth-averaged models, is to locally increase the bottom roughness or add an additional bottom shear stress term for vegetated regions. (e.g. Chen *et al.* (2007)). The second method is to include a sink term into the momentum equations for fluid motion based on the expected bulk drag produced by the vegetation. In estimating the resistance to the flow, quantities like the stem diameter, spacing, and height are needed, as well as an estimate of the drag force produced by a single stem, and the determination of a drag coefficient is required. In steady current environments, where the estimation of flow reduction is important for estimating riverine hydrodynamics and channel stability, a variety of experiments have been performed to investigate the hydrodynamics through vegetation, with the pioneering work being performed by Nepf (1999). In wave environments, Dalrymple *et al.* (1984) proposed a formulation to model the energy dissipation provided by an array of cylinders and the resultant reduction of the wave height. This formulation considers the estimate of the drag coefficient on an individual cylinder, the height

of the vegetation, the vegetation density, and the wave characteristics (phase speed, wave number, group speed, and water depth). Using this formulation with their newly obtained laboratory data, Augustin *et al.* (2009) found that the bulk drag coefficient scaled well with the Reynolds number for emergent vegetation, but near-emergent vegetation varied more with the Keulegan-Carpenter number (generally defined as $KC = U_w T/D$ where T is the wave period and U_w is some wave velocity scale often assumed as the maximum velocity, and D is a representative diameter). However, there was considerable scatter in the drag coefficient estimates, and real vegetation was not considered.

This research has focused on the estimation of wave height reduction due to the presence of vegetation in coastal environments. This is accomplished through the continued analysis of data collected during the summer of 2010 from a laboratory experiment at Oregon State University. Data collected at this experiment are unique, as real, flexible vegetation was used in a variety of wave conditions.

Methodology

During the summer of 2010, PI Smith and her graduate students participated in a NSF funded experiment at the O. H. Hinsdale Wave Research Laboratory at Oregon State University. The original study "Ecological modeling of emergent vegetation for sustaining wetlands in high wave energy coastal environments" was proposed by Dr. Daniel Cox and Dr. Denny Ablert at Oregon State University. LSU's participation was supported by the Louisiana Board of Regents and the Louisiana Water Resources Research Institute. The experiment was performed in the Large Wave Flume, which is 104 m long, 3.7 m wide, and 4.6 m deep. The recently upgraded wavemaker is capable of generating regular and random waves with wave heights up to 1.8 m and wave periods of 4 to 7 seconds. This is the only flume in the United States capable of creating these near-field scale conditions.

The flume was divided into four, 10 m long channels as shown in Figure 1(a). Three of the four channels were planted with bulrush (*Schoeneplectus pungens*), which is a fairly common species of wetland vegetation growing throughout the United States. Bulrush is a perennial species with the stem having a triangular cross-section for most of the upper part with a circular cross-section at the base. The vegetation used in the experiment were harvested from young natural bulrush beds in the Tillamook Bay of Oregon in the late spring of 2009. The bulrush stems with their root system still intact were cut out in blocks from the inner estuarine regions experiencing low to moderate wave forcing similar to what was simulated in the laboratory. These were then placed in the specially constructed channel boxes and careful preparation was undertaken to sustain their growth throughout the winter of 2009 in the laboratory. The purpose of this exercise was to mimic the field conditions in the best possible way. Two of the channels (B and D) had a nearly identical vegetation distribution, while the bulrush in channel C was less dense and slightly shorter. Channel A was setup as a sand channel to be used as a control for the experiment.

Wave gauges were placed at the leading edge of each channel and on a moveable platform. This allowed for the observation of the free surface at a variety of locations within the channels. During the three-week experiment, over 200 wave trials were run for the measurement of wave attenuation, and nearly 100 wave trials were run for the investigation of the velocity and turbulence characteristics within the vegetation. The results descibed here are for wave

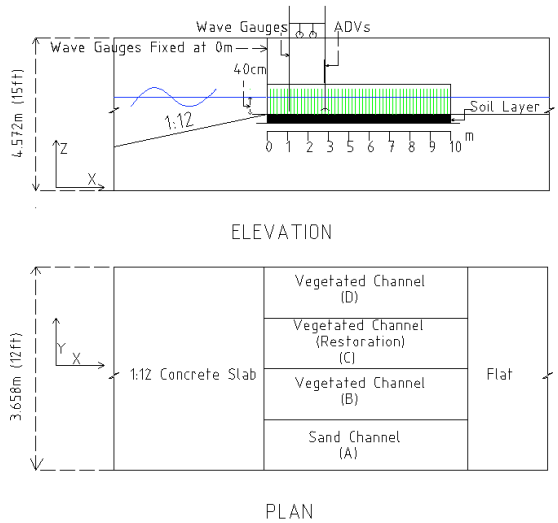

Figure 1: Experimental setup in the Large Wave Flume. Figure is not to scale.

runs with a 40 cm water depth, leading to fully emergent vegetation. Wave heights of 5-15 cm and wave periods of 1-3 s were considered, which are typically of estuarine waves.

Results

Wave height decay by vegetation is quantified using the wave transmission coefficient $K(x)$ which is defined as a function of wave height $H(x)$ (Dalrymple *et al.*, 1984) as

$$K(x) = \frac{H(x)}{H(0)} \tag{1}$$

where $H(0)$ is the incident wave height at the channel entrance and x is the shoreward distance from the incident wave height location. As all the wave cases were regular waves $H(x)$ and $H(0)$ were both taken as mean wave heights calculated using a zero-crossing method (Tucker and Pitt, 2001) from the water surface elevation time series at the wave gauge (WG) location. While computing K using Eqn. 1, the water surface elevation time series at the x location was properly time-lagged with the same at the 0 m location so that the wave heights calculated from the representative interval at the two locations were comparable.

Using Eqn. 1, the wave transmission coefficients were calculated for the two channels for each of the wave cases and at each location of the WG cart. Figure 2 shows the variation of K with x for a variety of wave cases from Experiments 1 to 3. Waves having the same mean wave heights but varying time periods are grouped together in different panels to study the effect of time period on wave attenuation. The topmost panel represents the cross-shore variation of attenuation for H_0=5 cm waves, the middle for H_0=10 cm cases and the bottom most panel for H_0=15 cm cases. A prevalent issue was that the K values in the sand channel oscillated within a given range for more or less all the three time period waves, with the T=2.0 s wave showing the greatest variability. One reason for the increase in wave heights in the sand channel may have been due to standing waves generated as a result of reflection from the back of the channel. Though padding material was placed at the back, some waves were found to be reflected into the sand channel. This was not a problem in the

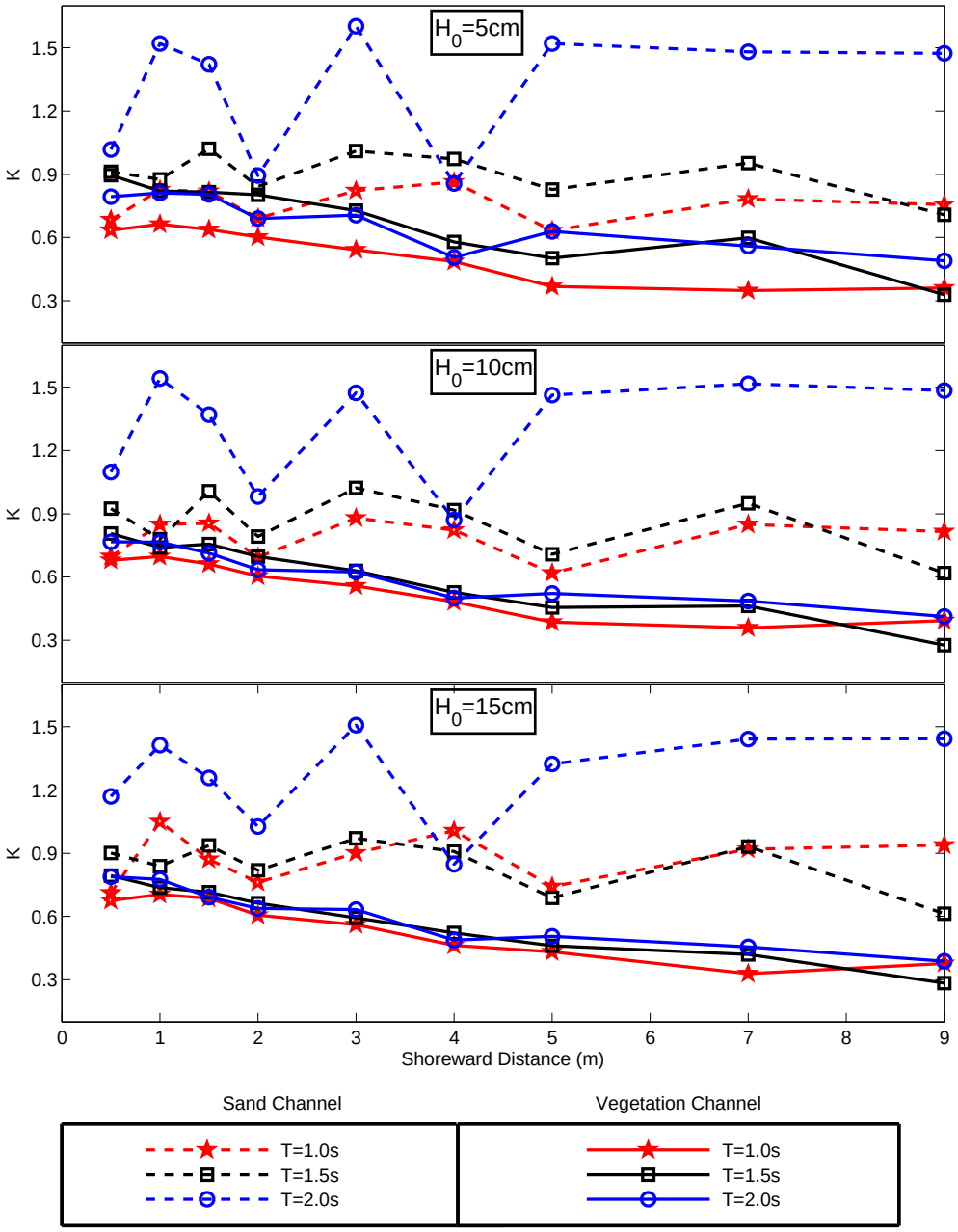

Figure 2: Effect of Time Period on Spatial Variation of Wave Attenuation

vegetation channel as most of the waves had attenuated by the time they reached the back of the flume. In spite of the variability however the sand channel attenuation remained fairly constant while the vegetation channel showed an almost exponential decrease in attenuation. The attenuation curves for the vegetation channel show that the attenuation for the T=1.0 s wave is greater than the T=1.5 s and T=2.0 s waves for the H_0=5 cm case, the difference however diminishing as H_0 increased to 15 cm. This may be because the increased frequency of flapping causes increased stalk-fluid interaction and hence increased dissipation of vortices. However at higher wave height, since the orbital velocities are already higher the increased flapping may not create any added dissipation to the already existing highly turbulent

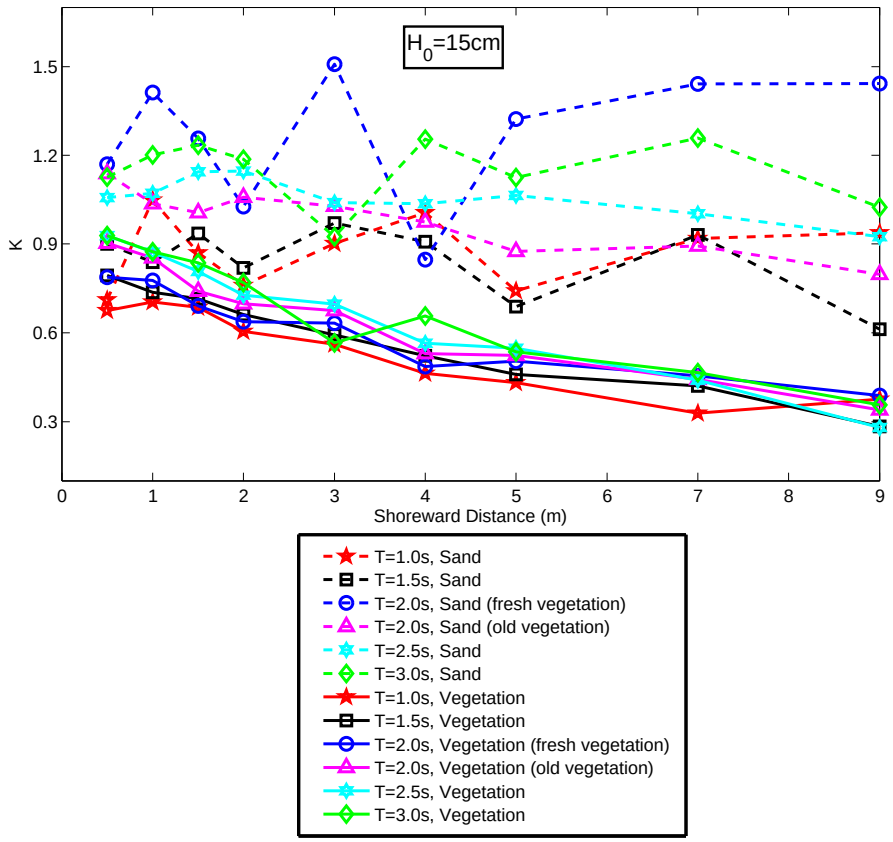

Figure 3: Spatial Variation of Wave Attenuation for H_0=15cm cases

shedding of vortices.

Figure 3 shows the variation of wave attenuation for a variety of waves with different time periods but a single deep water wave height of H_0=15 cm. Here also it is seen that under the same wave energy condition the T=1.0 s waves have the highest dissipation reiterating the fact discussed before. In addition it can be seen that Figure 3 presents two sets of trials of the same T=2.0 s wave, one labeled 'fresh vegetation' and the other as 'old vegetation'. These two sets differed in that they were conducted over a week in between them, the 'fresh vegetation' trial-set is one that was conducted earlier and a separate series of wave experiments (whose results are not in the scope of this thesis) were run in between the week so that the vegetation for the latter trial-set ('old vegetation') became less stiff, with the emergent portion of the stem laid flat across the water surface. This loss of stiffness is attributed to a combination of repeated exposure to wave forcing as well as the lack of natural light to sustain growth. Looking at the attenuation curves for the vegetation channel the fresh versus old effect can be seen in that for the old vegetation the attenuation decreased towards the front portion of the channel up to almost 7 m after which the attenuation increased slightly possibly due to the almost complete slanting of the stalks which increased the submerged portion of the above ground biomass, thereby increasing turbulence within the water column. However the difference between the two records were relatively minor compared to the variation with wave period.

Drag Coefficient Variations

Dalrymple *et al.* (1984) use a conservation of energy approach to equate the rate of wave energy decay in the shoreward direction to the energy dissipation due to work done on the plant stems by the waves. Using this approach and assuming linear wave theory holds, the drag coefficient can be related to the wave attenuation factor by,

$$\alpha = \frac{g^2 C_d d H(0) N[cosh^2(ks) + 2] sinh(ks)}{9\pi k C_G C^3 cosh^3(kh)} \tag{2}$$

where the factor α occurs in the attenuation factor as,

$$K = \frac{H(x)}{H(0)} = \frac{1}{1 + \alpha x} \tag{3}$$

Here, C_d is the drag coefficient for an individual plant stem, N is the plant stem density calculated as number of plants per unit area, d is the plant stem diameter, s is the submerged height of plants and for our case is equal to the depth h as all experiments were conducted in emergent conditions, $k = 2\pi/L$ is the wave number, L being the wavelength calculated iteratively using the dispersion relationship $L_0 = Ltanh(kh)$, $L_0 = gT^2/2\pi$ being the deepwater wavelength, g the acceleration due to gravity, $C_G = nC$ is wave group velocity, where $n = 0.5[1 + 2kh/sinh(2kh)]$ and $C = L/T$ is wave phase speed. The plant density (N) for the vegetation channel was known as 1202 stems/m^2 from sampling studies performed during the course of the experiment. A median stem diameter was obtained from the same sampling study and was found to be 4 mm. The regular wave characteristics being known for each trial, the remaining parameters in Eqn. 2 were calculated assuming linear wave theory applies.

The Reynolds number (Re) and Keulegan Carpenter number (KC) with respect to the stem diameter (d) and the maximum orbital velocity (u_{max}), calculated at the free surface are,

$$Re = \frac{u_{max} d}{\nu} \tag{4}$$

and,

$$KC = \frac{u_{max} T}{d} \tag{5}$$

where T is the wave period for any particular wave case and ν is the kinematic viscosity of water assumed as $10^{-6} m^2/s$. Another parameter (β), called the Viscous Frequency Parameter can be defined as,

$$\beta = \frac{Re}{KC} = \frac{d^2}{\nu T} \tag{6}$$

Figure 4 represents the dependence of C_d with stem Re (top panel), KC (middle panel) and β (bottom panel) with the different wave cases separated in order to understand the contribution of different wave conditions on C_d. In general, both C_d versus Re and C_d versus KC plots show a decrease in drag coefficient with increase in Re and KC. This shows that under increased turbulence the drag coefficient decreases. In terms of H_0 it is seen that there are distinct ranges of C_d with various Re regimes, the H_0=5 cm waves typically have

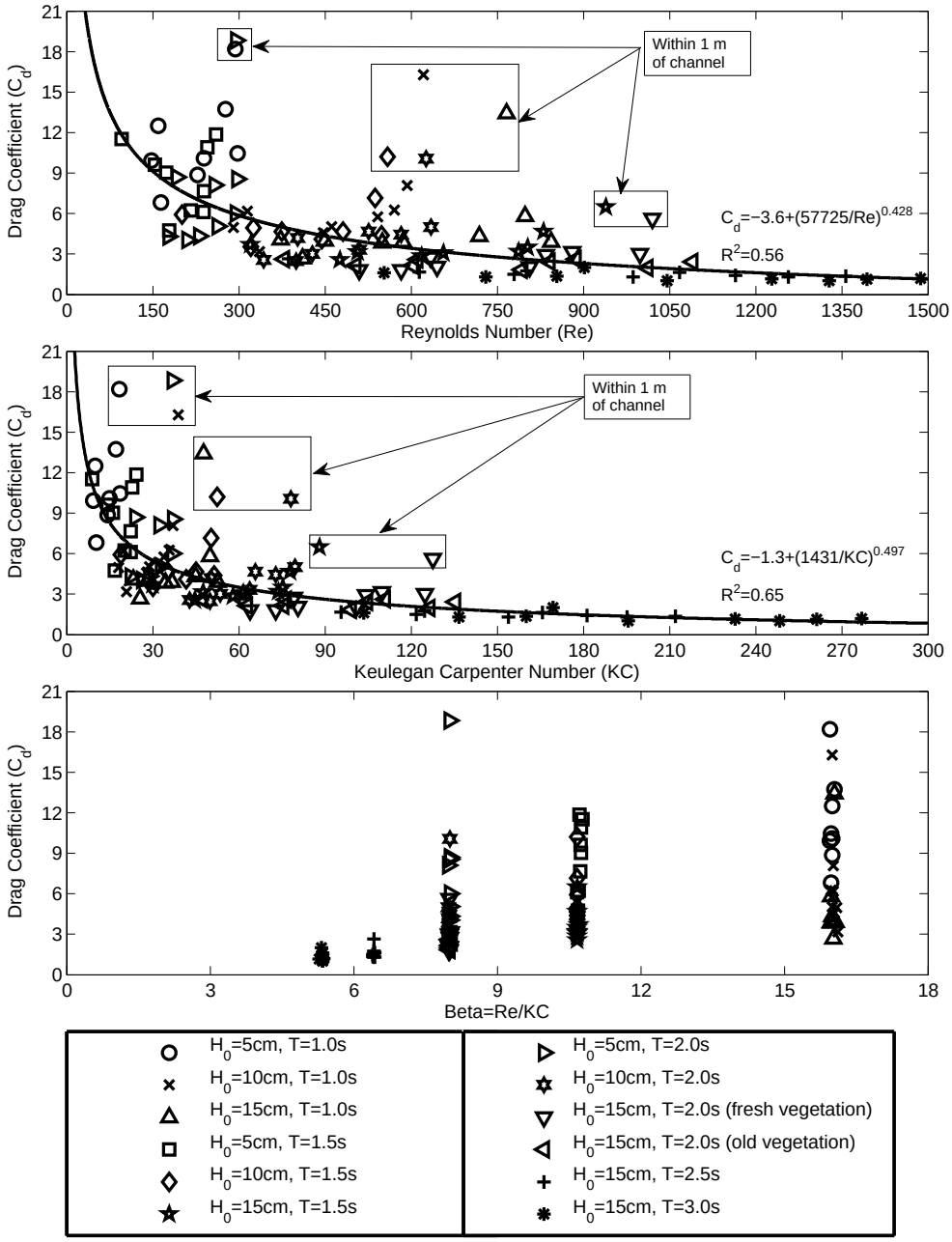

Figure 4: Variation of Drag Coefficient with Re, KC and β for Different Wave Cases

$3 < C_d < 15$ with Re regime $75 < Re < 300$, the H_0=10 cm waves have $1.5 < C_d < 6$ with Re regime $300 < Re < 700$ and the H_0=15 cm waves have $1 < C_d < 1.5$ with Re regime $750 < Re < 1500$. The relative scatter in the data is relatively higher at lower H_0 than in higher ones. Thus C_d increases with β, which means that drag coefficient is higher for lower time periods as was observed in previous sections, with C_d being tightly grouped at specific β points showing that there was no significant frequency shift among trials. These observations are consistent with those of other researchers (Kobayashi *et al.*, 1993; Mendez and Losada, 1999; Augustin *et al.*, 2009) who worked with artificial vegetations. It is to be noted that the Re for the cases considered by the foregoing researchers were much higher

than the ones considered here, typically greater than 3000 due to the thicker artificial stems used in their experiments.

Following the work of Kobayashi *et al.* (1993) and Mendez and Losada (1999), equations of the type

$$C_d = a + \left(\frac{b}{Re}\right)^c \tag{7}$$

are fit to the calibrated C_d values from the artificial submerged kelp experiments of Asano *et al.* (1988) and obtained values of the coefficients for rigid plants (Kobayashi *et al.*, 1993) (applicable in the range $2200 < Re < 18,000$) and (Mendez and Losada, 1999) (range $200 < Re < 15,500$) as well as flexible plants (Mendez and Losada, 1999) (range $2300 < Re < 20,000$). If these equations are extended to the Re range observed here, it yields C_d values much greater than the ones observed and thus are not applicable to our range of Re. Kobayashi *et al.* (1993) and Mendez and Losada (1999) results being based on submerged vegetation experiments, their C_d values are expected to be lower than those from the present set of experiments where emergent condition prevailed. Though Augustin *et al.* (2009) results are from emergent vegetation experiments, the high Re conditions in their experiments probably gave lesser C_d values and was also the reason why in spite of their KC values overlapping with those in our experiments, our C_d values were higher than their values. Efforts to fit an equation of the type Eqn. 7 after screening out some of the 'outlier' points (9 outliers out of 108 data points) in the entire range of the Re did not yield very good correlation with our data (Figure 4). However the correlation with KC was somewhat better. The most important reason for the failure to fit such an equation had to do with the fact that there was too much of scatter and looking at Figure 4 it is seen that most of the scatter points and also the 'outliers' are due to high C_d values that occurred towards the first 0 to 1 m of the channel. As was discussed before it is not clear exactly what caused the increased values of C_d at the beginning of the channel and the complex dynamics occurring in the first 1 m may not actually relate to equations of type of Eqn. 7 and is an open avenue for future work.

Conclusions

Wave attenuation effects of the vegetation channel was found to be significant, with a wave transmission coefficient for the vegetated channel decaying in almost an exponential manner, while that in the sand channel remained more or less constant as waves progressed through the channels. Nearly 40% of the wave energy was attenuated in the first 3 m of the vegetated channel. In general for a given wave period, attenuation was nearly independent of wave height, except for the 5 cm wave which showed comparatively decreased attenuation for $T = 1.5$ s. For a given wave height it was found that lower time periods had greater attenuation and indicate that greater the frequency of flapping the higher is the attenuation.

The drag coefficient, calculated from the conservation of energy approach and assuming linear wave theory, was compared with distance within the channel and was found to decrease exponentially within the first 2 meters into the channel, after which drag coefficient remained almost constant. The high values of drag coefficient towards the beginning of the channel could not be explained using the conservation of energy approach and further research will be done in the future to isolate the effects causing this phenomenon. Two reasons

are proposed for the high values, one is that there may be other attenuation forces at play towarrds the beginning of the channel, which is creating increased decay in wave heights over a short distance and thereby increased drag and the other is that the uncertainity in the measurement of the stem density and median plant diameter, which for natural vegetation stems have been found to vary widely in the field, is producing highly varying C_d values. Drag coefficient decreased with increasing wave height and time period suggesting decreased drag at turbulent conditions. Comparisons of C_d with Reynolds number and Keulegan Carpenter number revealed a decrease in drag coefficient with both the parameters. Efforts were made to fit a exponential type curve in the lines of Kobayashi *et al.* (1993) and Mendez and Losada (1999) and though a best fit equation was obtained the correlation was not very good due the greater degree of scatter which stressed the fact that for a complete description of the drag coefficient of natural, flapping vegetations it is important to relate it with the flapping mechanism. This was also the first attempt to obtain drag coefficients at such small Reynolds number regime as most researchers before have worked on higher Reynolds number regions due to their use of thicker artificial stems. The correlation with Keulegan Carpenter number was slightly better while drag coefficient increased with increasing β parameter indicating clear wave period dependence. There were video footage of vegetation flapping collected at the time of the experiment which were not presented here, but may be used to relate the flapping to the drag coefficient in future studies.

As part of this funding, Mr. Agnimitro Chakrabarti completed his M.S. in Civil Engineering. This work was also presented at the 2012 American Geophysical Union's Ocean Sciences Meeting.

References

Asano, T., Tsutsui, S., and Sakai, T. (1988). Wave damping characteristics due to seaweed. *Proc. 35th Coast. Eng. Conf. in Japan (in Japanese), JSCE*, pages 138–142.

Augustin, L. N., Irish, J. L., and Lynett, P. (2009). Laboratory and numerical studies of wave damping by emergent and near-emergent vegetation. *Coast. Eng.*, 56(3):332–340.

Chen, S.-N., Sanford, L. P., Koch, E. W., Shi, F., and North, E. W. (2007). A nearshore model to investigate the effects of seagrass bed geometry on wave attenuation and suspended sediment transport. *Est. Coast.*, 30(2):296–310.

Dalrymple, R. A., Kirby, J. T., and Hwang, P. A. (1984). Wave diffraction due to areas of energy dissipation. *J. Waterw., Port, Coastal, Ocean Eng., ASCE*, 110(1):67–79.

Kobayashi, N., Baichle, A. W., and Asano, T. (1993). Wave attenuation by vegetation. *J. Waterw., Port, Coastal, Ocean Eng., ASCE*, 119(1):30–48.

Mendez, F. J. and Losada, I. J. (1999). Hydrodynamics of a vegetation field induced by wind waves. *J. Geophys. Res.*, 104(C8):18,383–18,396.

Nepf, H. M. (1999). Drag, turbulence, and diffusion in flow through emergent vegetation. *Water Resour. Res.*, 35(2):479–489.

Tucker, M. J. and Pitt, E. G. (2001). *Waves in ocean engineering.* Elsevier.

Information Transfer Program Introduction

Because of the Deepwater Horizon oil spill, our efforts for information transfer were dominated by that activity again in FY 2011. Full details are provided in the “Notable Achievements” section of the report. Highlights of our activities are listed below:

LWRRI built and managed a collaborative web review process for the Deep Water Horizon Science and Engineering Review Team immediately after the spill. This allowed for rapid review of dozens of documents and storage of GB’s of information for review by statewide academic members of the team. This activity continued into FY 2011.

LWRRI participated in LSU’s institutional response to the spill including participation in group meetings with Lisa Jackson, Head of EPA and Jane Lubchenko, Head of NOAA and private meeting with Paul Anastas, Head of EPA's Office of Research and Development.

LWRRI participated in organizing scientific conferences and symposia related to DH Spill (Steering committee of SETAC Focused Oil Spill Conference to be held in Pensacola, FL in April 2011; chairing session at Battelle Bioremediation Conference in Reno, NV in June 2011).

LWRRI is coordinating research and damage assessment for the Wisner Donation property in Lafourche Parish, one of the 10 largest landowners in the state. The Wisner Donation property includes 35,000 acres including Fourchon Beach.

LWRRI is working with Point au Chiene tribe in understanding impacts from DH spill on marshes in Barataria Basin, LA.

LWRRI was the chief sponsor of the LSU Environmental Film Series in March and April 2011 at LSU. The following films included: Troubled Waters, GasLand and Wasteland. These films were followed by discussions with students and faculty organized by LWRRI. Attendance averaged 120 per night.

In addition, the 104B funded one information transfer project, 2011LA80B, Louisiana Watershed Education Initiative for Environmental Sustainability from Z-Q Deng. The results of this project are presented below.

Louisiana Watershed Education Initiative for Environmental Sustainability

Basic Information

Title:	Louisiana Watershed Education Initiative for Environmental Sustainability
Project Number:	2011LA80B
Start Date:	3/1/2011
End Date:	2/28/2012
Funding Source:	104B
Congressional District:	6th
Research Category:	Not Applicable
Focus Category:	Education, Models, Non Point Pollution
Descriptors:	None
Principal Investigators:	Zhi-Qiang Deng

Publications

1. Deng, Z.-Q. and Patil, A. (2011). “Assessment of water quality variation in Amite River watershed under changing climate and land use.” In: Water Quality: Current Trends and Expected Climate Change Impacts, IAHS Publ. 348, 2011.
2. Patil, A. and Deng, Z.-Q. (2012). “Input-data measurement induced uncertainty in watershed modeling.” Hydrological Sciences Journal, 57(1), 118-133.
3. Patil, A. and Deng, Z.-Q. (2012). “Temporal Scale Effect of Loading Data on Instream Nitrate-Nitrogen Load Computation.” Water Science and Technology (in press), DOI: 10.2166/wst.2012.163.

Louisiana Watershed Education Initiative for Environmental Sustainability

BASIC INFORMATION

Title:	Louisiana Watershed Education Initiative for Environmental Sustainability
Project Number:	2011LA80B
Start Date:	3/01/2011
End Date:	2/28/2012
Funding Source:	104B
Congressional District:	6th
Research Category:	Watershed Education
Focus Category:	Education, Models, Non Point Pollution
Descriptors:	Environmental Sustainability, Nonpoint Source Pollution, Watershed Excellence
Principal Investigators:	Zhi-Qiang Deng

RESEARCH AND EDUCATION

Problem and Research Objectives

The Federal Clean Water Act (CWA) has played a major role over the past 40 years in controlling point pollution sources through a system of laws, regulations and judicial enforcement. However, land use/land cover change along with climate change has significantly increased nonpoint source pollution. The pollutants from the nonpoint sources are difficult to measure and nearly impossible to regulate through the conventional CWA-based approach alone. The solution to the nonpoint source pollution demands a watershed approach that looks broadly to maintain water quality and ecological integrity on a watershed basis in the context of environmental sustainability. The implementation of the watershed approach requires a combination of public education, scientific endeavors, water quality management, and regulatory enforcement. This is a critical regional and state water quality problem needing to be addressed.

The overall goal of this project is to promote the application of watershed approach and thereby the watershed excellence in Louisiana by initiating a watershed education program, called Louisiana Watershed Education & Training Program for Environmental Sustainability (LA WETPES). Specific objectives of the project are: (1) To provide local residents with information on the quality of their watershed and solutions to their watershed pollution problems, enhancing the development and growth of local stakeholder involvement in the Watershed Excellence program in Louisiana; (2) To provide training and technical assistance on topics of concern or interest to local watershed stakeholders and more specifically on the application of well-calibrated watershed models for water resources and environmental managers and engineers; and (3) To increase the future workforce equipped with the skills necessary to apply the watershed approach in civil and environmental engineering.

Methodology

The objectives have been accomplished by executing three tasks: (1) construction of a user-friendly website for LA WETPES, (2) making well-calibrated and validated watershed models available for potential users/modelers and providing on-demand professional training for watershed model applications; and (3) organization of a summer watershed internship program for primarily undergraduate students while the program is also open to graduate students and water resources professionals. The proposed strategy is to expose local stakeholders in a variety of watershed education settings including web visits, field trips, hands-on experiences, and seminars supported by the scientific endeavors of PI's research group.

The proposed project has broader implications for environmental restoration and sustainability in Louisiana. This project will help water resources communities identify nonpoint source pollution problems in Louisiana watersheds and find LID (Low Impact Development) based solutions to restoration of impaired waterbodies through a watershed approach while educating/training the next generation of water resource and environmental engineering professionals. This project is the first step toward the establishment of a US EPA designated Center for Watershed Excellence in Louisiana.

PRINCIPAL FINDINGS AND SIGNIFICANCE

1. Construction of Website for Louisiana Watershed Education & Training Program for Environmental Sustainability (LA WETPES website)

The LA WETPES website can be accessed directly via the web link: http://www.cee.lsu.edu/people/Deng/resources.html or indirectly by clicking the "Resources" tab on the Deng Research Group website: http://www.cee.lsu.edu/people/Deng/index.html

The LA WETPES website contains six sections, including (1) What Is A Watershed?, (2) Louisiana Watersheds, (3) Watershed Functions, (4) Watershed Processes, (5) Watershed Approach, and (6) Watershed Modeling. The LA WETPES website is intended to serve as the premier local resource: the One-Stop Shop for Louisiana watersheds. The following are some screen captures of the LA WETPES website:

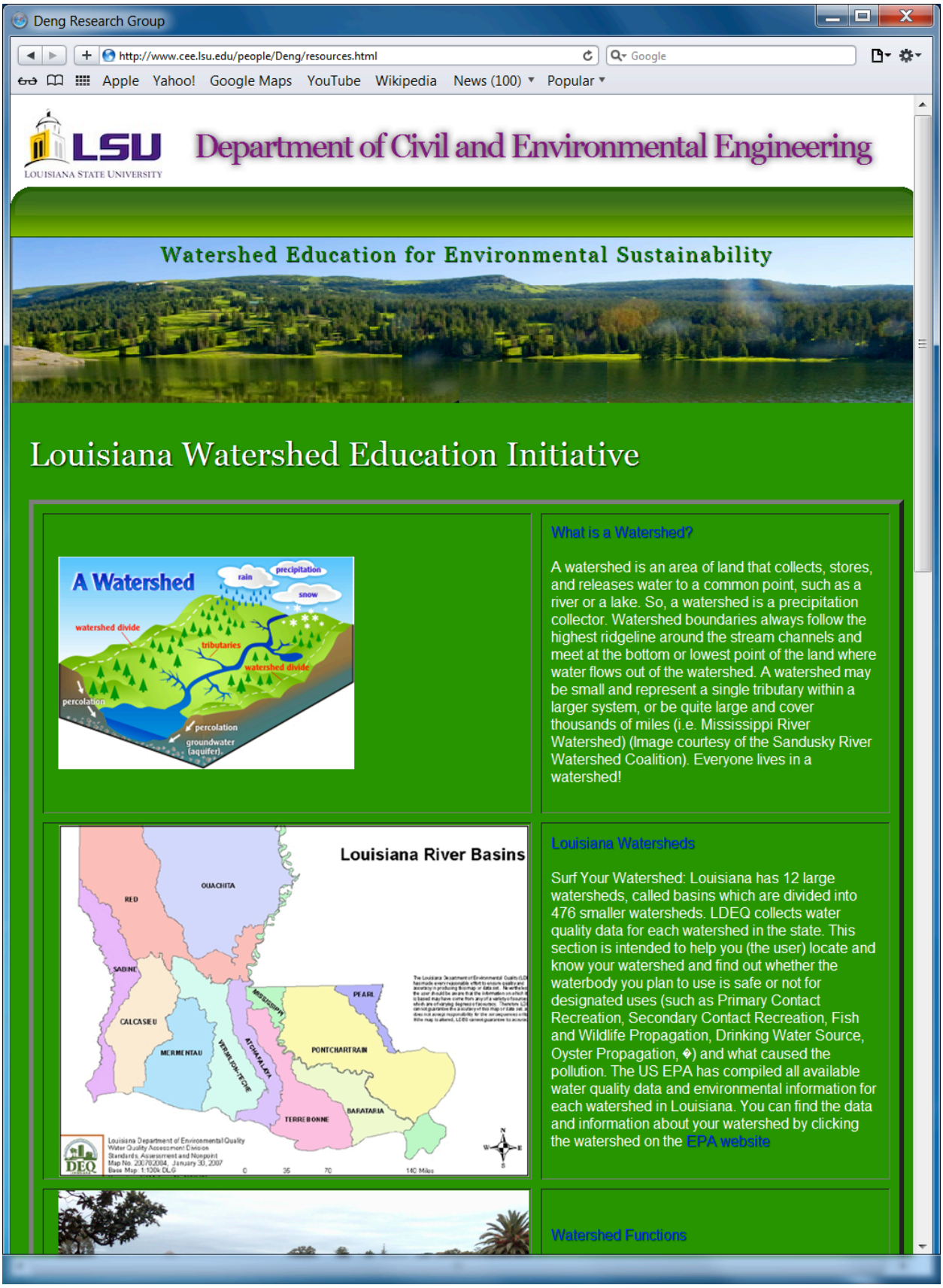
Deng Research Group
http://www.cee.lsu.edu/people/Deng/resources.html
Apple Yahoo! Google Maps YouTube Wikipedia News (100) Popular
LSU
LOUISIANA STATE UNIVERSITY
Department of Civil and Environmental Engineering
Watershed Education for Environmental Sustainability
Louisiana Watershed Education Initiative
A Watershed
rain
precipitation
snow
watershed divide
tributaries
watershed divide
percolation
percolation
groundwater (aquifer).
What is a Watershed?
A watershed is an area of land that collects, stores, and releases water to a common point, such as a river or a lake. So, a watershed is a precipitation collector. Watershed boundaries always follow the highest ridgeline around the stream channels and meet at the bottom or lowest point of the land where water flows out of the watershed. A watershed may be small and represent a single tributary within a larger system, or be quite large and cover thousands of miles (i.e. Mississippi River Watershed) (Image courtesy of the Sandusky River Watershed Coalition). Everyone lives in a watershed!
Louisiana River Basins
RED
OUACHITA
SABINE
CALCASIEU
MERMENTAU
MISSISSIPPI
VERMILION-TECHE
ATCHAFALAYA
PEARL
PONTCHARTRAIN
TERREBONNE
BARATARIA
Louisiana Department of Environmental Quality
Water Quality Assessment Division
Standards, Assessment and Nonpoint
DEQ
Louisiana River Basins
What is a Watershed?
Louisiana Watersheds
Surf Your Watershed: Louisiana has 12 large watersheds, called basins which are divided into 476 smaller watersheds. LDEQ collects water quality data for each watershed in the state. This section is intended to help you (the user) locate and know your watershed and find out whether the waterbody you plan to use is safe or not for designated uses (such as Primary Contact Recreation, Secondary Contact Recreation, Fish and Wildlife Propagation, Drinking Water Source, Oyster Propagation,) and what caused the pollution. The US EPA has compiled all available water quality data and environmental information for each watershed in Louisiana. You can find the data and information about your watershed by clicking the watershed on the EPA website
Watershed Functions

Deng Research Group

http://www.cee.lsu.edu/people/Deng/resources.html

Apple Yahoo! Google Maps YouTube Wikipedia News (100) Popular

Watershed Functions

Hydrological Functions: (1) Collection Function - It collects water from rainfall, snowmelt, and storage that becomes runoff, (2) Storage Function - It stores water of various amounts and for different durations, and (3) Discharge Function - It releases water as runoff.
Ecological Functions: (1) Water Quality Restoration Function - It provides diverse sites for biogeochemical reactions to take place and thereby removes contaminants and nutrients in water bodies; and (2) Habitat Function - It provides habitat for the flora and fauna that constitute the biological elements of ecosystems.

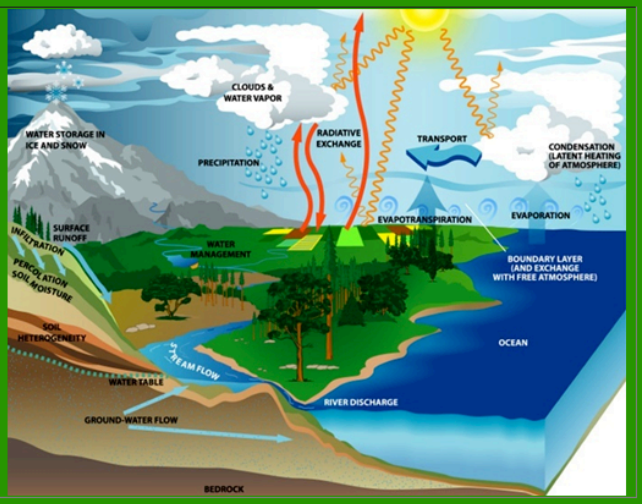

Watershed Processes

Typical watershed processes include precipitation, evapotranspiration, radiation exchange, interception, storage (upper and lower zone), surface runoff, infiltration, groundwater percolation, interflow, groundwater/base flow, sediment erosion and transport, soute transport, dispersion and diffusion, biogeochemical reactions, and land use/land cover changes. (Image courtesy of the USGS).

Watershed Approach

The Federal Clean Water Act (CWA) has played a major role over the past 40 years in controlling point pollution sources through a system of laws, regulations and judicial enforcement. However, land use/land cover change along with climate change has significantly increased nonpoint source pollution. The pollutants from the nonpoint sources are difficult to measure and nearly impossible to regulate through the conventional CWA-based approach alone. The solution to the nonpoint source pollution demands a watershed approach that looks broadly to maintain water quality and ecological integrity on a watershed basis in the context of environmental sustainability. The implementation of the watershed approach requires a combination of public education, scientific endeavors, water quality management, and regulatory enforcement.You may find more information about the watershed approach from the EPA website

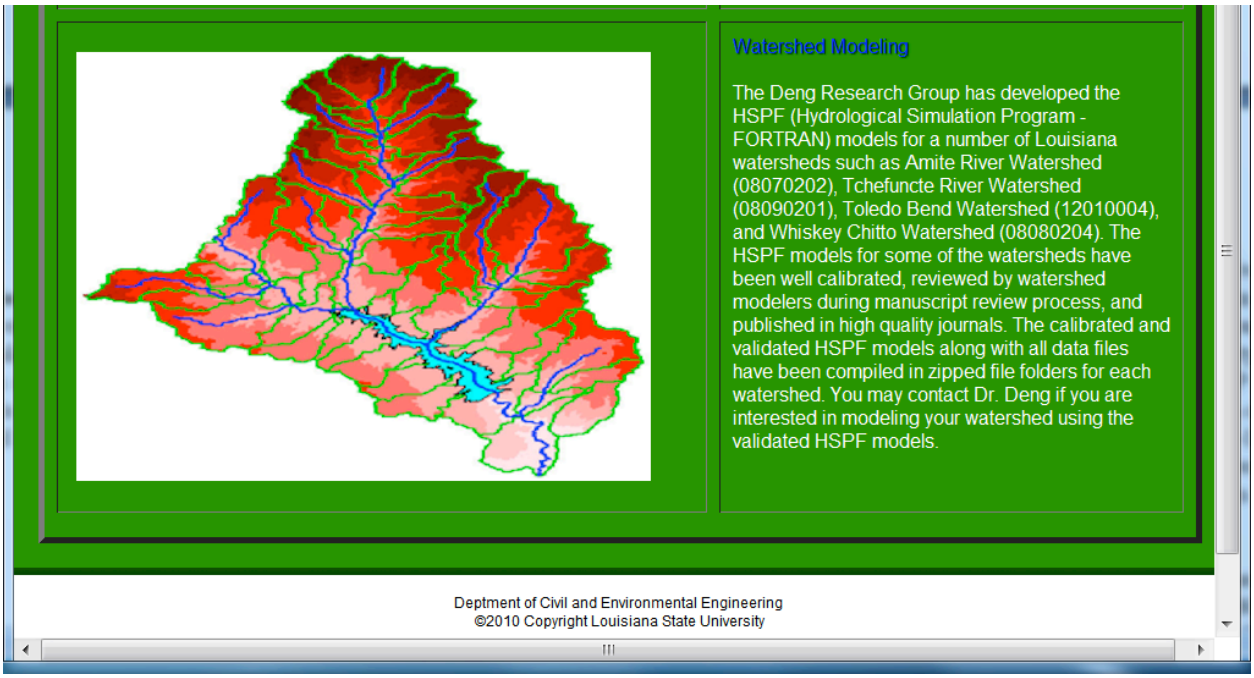

2. Calibration and Validation of Watershed Models and Modeling Support

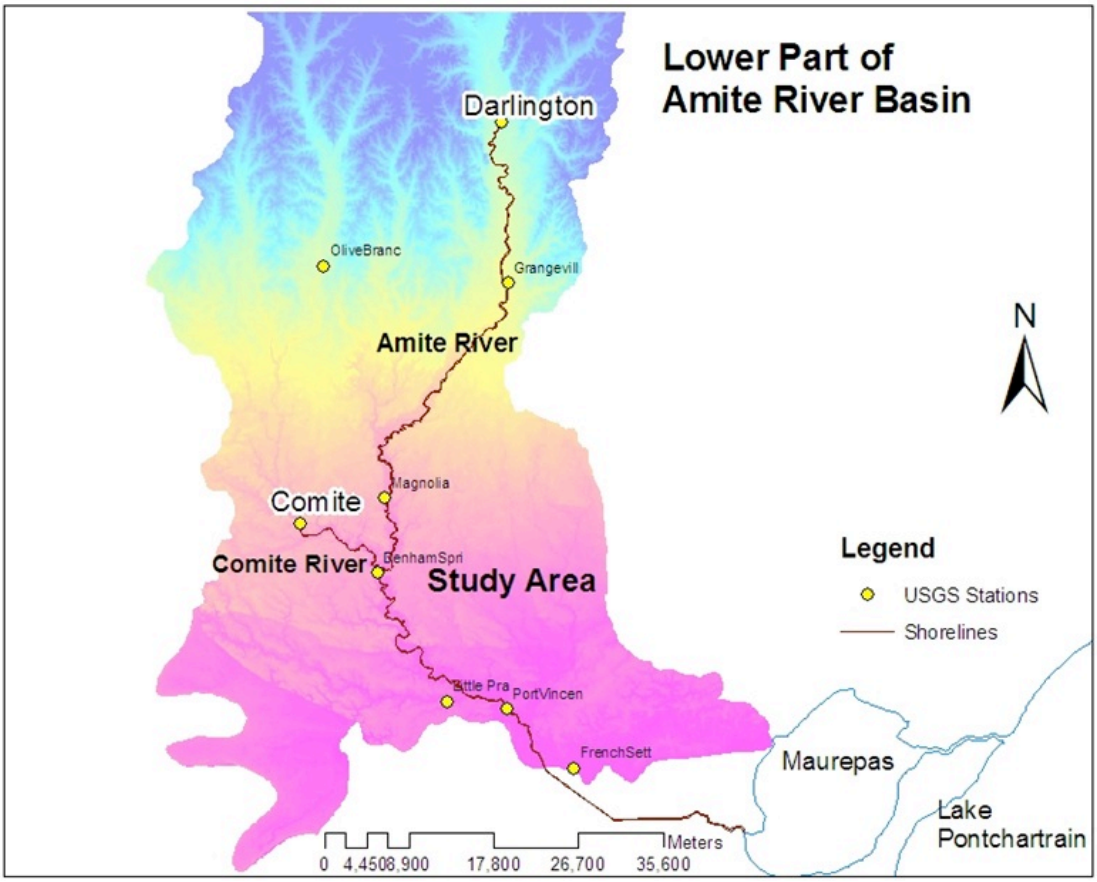

(1) **Amite River Watershed:** HSPF models have been developed, calibrated, and validated for the Amite River Watershed (08070202) for simulation of climate change effects (Paper 1), flow (Paper 3), instream dissolved oxygen changes (Papers 1 and 2), and nitrate-nitrogen loading (Papers 2 and 3). The models can be applied to develop and implement TMDLs for the Amite River Watershed for various contaminants and nutrients.

(2) **Tchefuncte River Watershed:** Modeling Effects of Urbanization and Agricultural BMPs on Phosphorus Loading in the Tchefuncte River Watershed.

A HSPF model has been calibrated and validated for the Tchefuncte River Watershed (08090201) in the Lake Pontchartrain river basin. The model was utilized to analyze the effects of urbanization and agricultural BMPs in the Tchefuncte River Watershed on phosphorus loading into the Lake Pontchartrain. It was found that (1) a total phosphorus load reduction of 23-59% is needed to meet the water quality standard in the Tchefuncte River watershed; (2) Agriculture dominated the input of ortho-P to surface waters in the Tchefuncte River Watershed (>96%); (3) Applying filter strips to 75% of the agricultural land in the watershed can potentially reduce ortho-P loading by 13-15%; and (4) increased urbanization (conversion of 25% of forested land to urban land) in the watershed may increase ortho-P loads by 5-15% and partially or entirely offset any improvements achieved by agricultural BMPs.

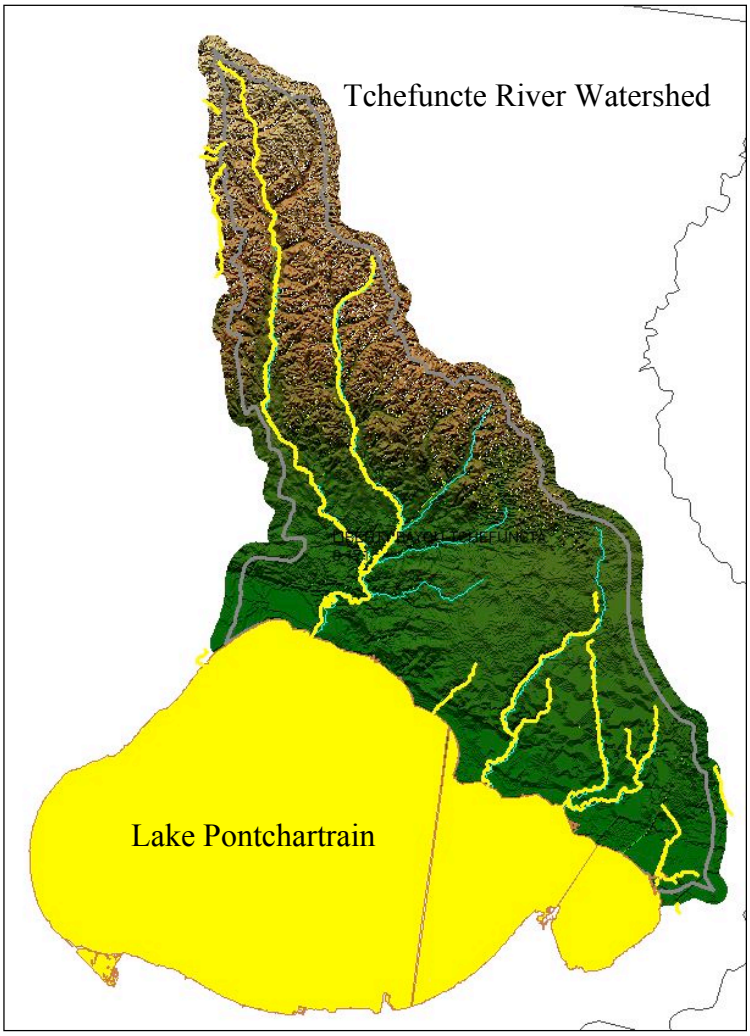

(3) **Whiskey Chitto Watershed:** A HSPF model has been constructed, calibrated and validated for the Whiskey Chitto Watershed (08080204) for the development of Total Maximum Daily Load (TMDL) for fecal coliform bacteria. It was found that (1) fecal coliform loads in Whiskey Chitto should be reduced by 27.72%t. During the winter season, the load should be reduced by 3.43% while the load should be reduced by 44.11% during summer season in the Whiskey Chitto watershed; and (2) After implementation of

BMPs, fecal coliform loads in summer season still need to be reduced by 16.30% in order to meet the water quality standard, though annual and winter season fecal coliform loads are meeting the water quality standard.

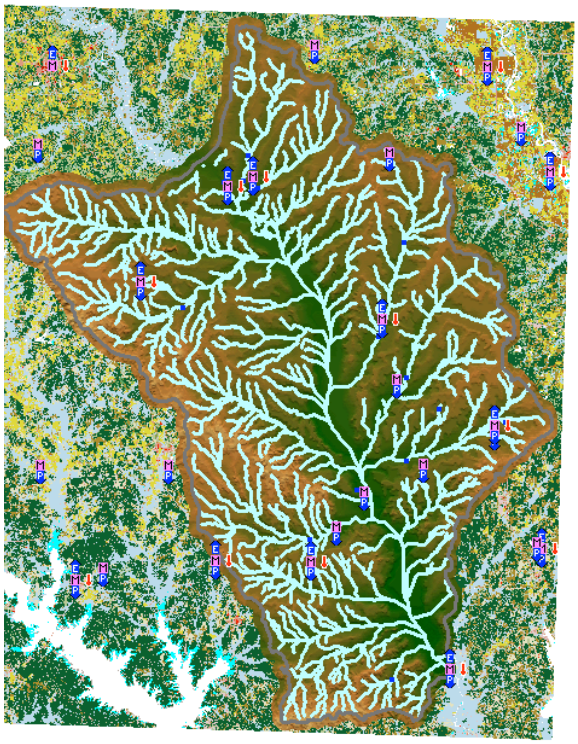

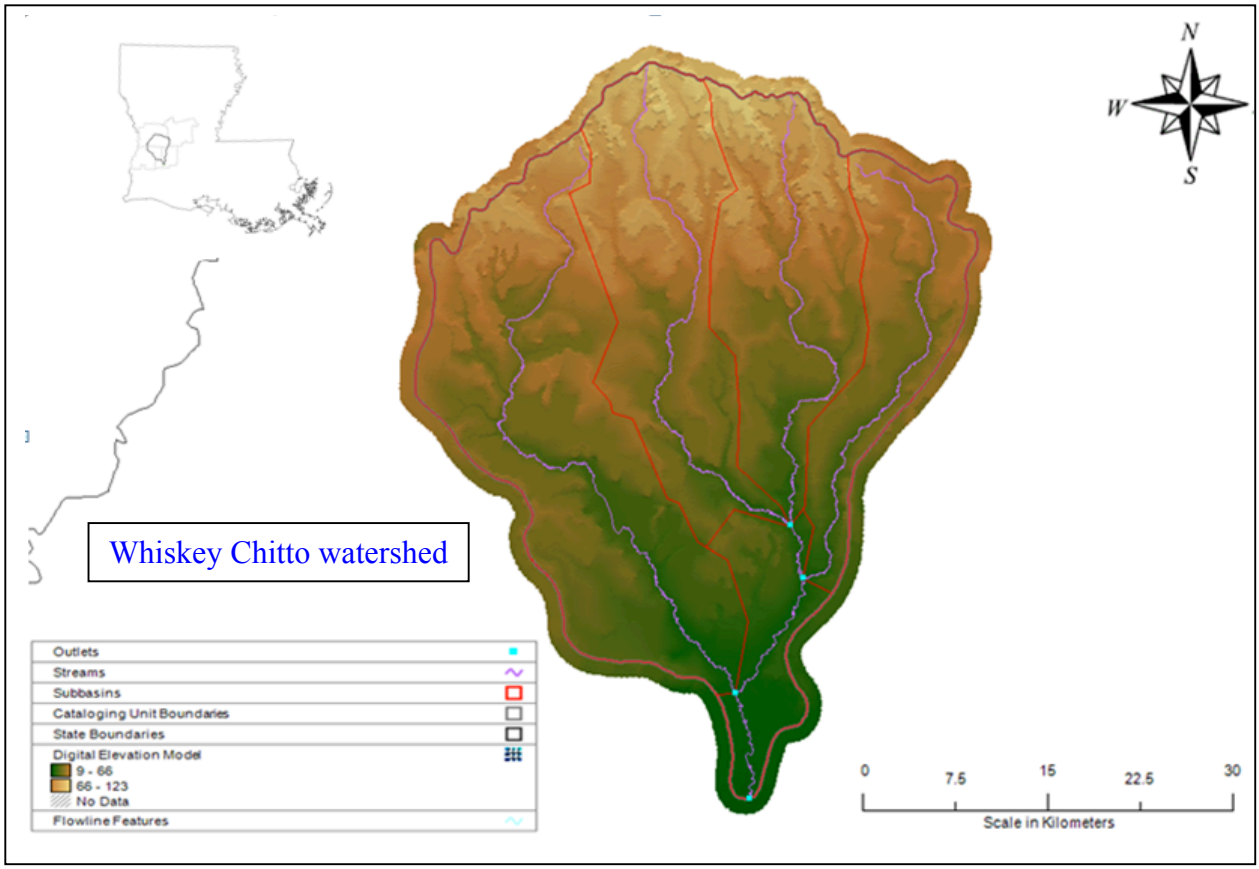

Toledo Bend Watershed (12010004)

(4) **Toledo Bend Watershed (12010004):** A HSPF model has been constructed, calibrated and validated for the Toledo Bend watershed (HUC 12010004) for the development of Total Maximum Daily Load (TMDL) for mercury. It was found that (1) soil erosion accounts for the vast majority of mercury pollution in the Toledo Bend reservoir; (2) point source discharges contribute a very small amount of the total mercury, and (3)

regional atmospheric deposition accounts for the remainder of the mercury found in the lake. Reducing the amount of mercury at point-source discharges is most likely not worth the effort, since stricter regulations at these discharge sites would not significantly affect the water quality related to mercury within the reservoir. Therefore, the most practical implementation of the mercury load reductions would be erosion control within the watershed and reaches. On the site scale, measures could be taken to prevent sediment from entering streams. BMP's such as silt fences, weir structures at site outfalls, and sediment traps in subsurface urban drainage channels could all be implemented throughout the watershed to reduce the amount of eroded sediment being routed to the Toledo Bend reservoir. On the subcatchment scale, rock weirs could be placed in streams or agricultural drainage ditches to trap sediment. Structures such as rock weirs should not pose a large threat to the hydrology of the region, since large flood events could simply short-circuit the weir and continue to flow while a portion of the particulate sediment would hopefully be trapped.

(5) **HSPF Model Training Workshop (on-demand professional training):** A workshop on Modeling Impact of Climate Change and Landuse Change on Water Resources was delivered by the PI on February 28, 2012 at the Southern University to demonstrate how different climate change scenarios will affect watershed ecosystem functions by changing watershed processes. Using the HSPF model Dr. Deng demonstrated to faculty (3) and students (30) of Southern University how a watershed modeling tool (Hydrological Simulation Program - FORTRAN (HSPF)) can be utilized to understand climate change impacts on watershed processes and ecosystem functions. The workshop demonstrated to the participants the utility of HSPF model by (1) introducing how the major components of HSPF work, and (2) showing modeling results of climate and land-use change impact on water resources (water quality and quantity) in the Amite River Watershed, Louisiana.

3. Implementation of Summer Watershed Internship Program

(1) The **Summer Watershed Education Program** was successfully conducted from May 23 – June 25, 2011 under the support of Remote Sensing & GIS Lab at Southern University, Baton Rouge. Eight minority students (4 from Southern University and 4 from LSU) participated in the summer internship program.

(2) The following picture shows the group of interns (plus 2 graduate students supporting the internship program) taking GPS data for our water quality sampling stations in the Lower Calcasieu Watershed (08080206) on June 18, 2011.

(3) The **Summer Watershed Internship Program** was highly appreciated by the interns. One of the interns commented that "Overall, the program was very informative. I really enjoyed being able to work with other women and engineers that were learning how to use the programs needed for our next generation of leaders. I feel like I will be better candidate for jobs in Louisiana… I would definitely recommend another internship like this to fellow students and would love to participate in one as well!" Some other comments include "I am so grateful to Dr. Deng (LSU) for having this class extended to students outside his department" and "Well taught and organized training. I earned lots in such a short time. Great Job!!" The quantitative evaluation rating of the program was 4.77/5.00 based on 7 evaluation criteria for the program.

INFORMATION TRANSFER

The user-friendly website for Louisiana Watershed Education & Training Program for Environmental Sustainability (LA WETPES) will be hosted in the LSU Department of Civil and Environmental Engineering and maintained by the PI. The LA WETPES website may also be

linked to the Louisiana Water Resources Research Institute (LWRRI) website http://www.lwrri.lsu.edu/ and to the website of the Louisiana Department of Environmental Quality (LDEQ): http://www.deq.louisiana.gov/portal/

USGS Summer Intern Program

None.

Student Support					
Category	**Section 104 Base Grant**	**Section 104 NCGP Award**	**NIWR-USGS Internship**	**Supplemental Awards**	**Total**
Undergraduate	6	0	0	0	6
Masters	1	0	0	0	1
Ph.D.	4	2	0	0	6
Post-Doc.	0	0	0	0	0
Total	11	2	0	0	13

Notable Awards and Achievements

Of note in FY2011 was LWRRI's participation in response to the Deepwater Horizon Oil Spill, the largest spill in US history. Details are presented below.

LWRRI advised response agencies

•Advised the state through the Horizon Science and Engineering Review Team (H-SERT), a group of academic experts who worked with state trustees on the response. LWRRI Director Pardue led one of the standing committees in H-SERT and participated by reviewing and commenting on dozens of documents and plans. LWRRI set up a collaborative web review process for H-SERT which allowed participating by academics across the state. Pardue also participated in helicopter tours with the lead trustee agency, the Office of Coastal Protection and Restoration. •Dr. Pardue also advised EPA on response and participated in meetings at LSU with Lisa Jackson, Head of EPA, Jane Lubchenko, Head of NOAA and Paul Anastas, EPA •Dr. Pardue has also provided comments on many plans and remediation strategies ongoing through 2012

LWRRI Conducted Research on the Spill

•LWRRI Director Pardue is coordinating research and damage assessment for the Wisner Donation property in Lafourche Parish, one of the 10 largest landowners in the state. The Wisner Donation property includes 35,000 acres including Fourchon Beach. Dr. Pardue has travelled to Wisner areas to conduct research an average of once per week since October 2010. •Received research funding from LSU GOMA BP fund and Wisner Donation •Ten students (undergraduate, MS and PhD) have been involved in this activity to date.

LWRRI organized conferences and presented research results

•Organizing scientific conferences and symposia related to DH Spill (Steering committee of SETAC Focused Oil Spill Conference to be held in Pensacola, FL in April 2011; chairing session at Battelle Bioremediation Conference in Reno, NV in June 2011 •Given numerous talks locally, regionally and nationally on the impacts of the spill